Review of the Microwave Instability

S. Heifets
heifets@slac.stanford.edu

Presented at the Workshop on Broadband Impedance Measurements&Modeling, SLAC, Stanford, February 28-March 2, 2000

Abstract:

Single bunch microwave instability (MWI) and relaxation oscillations have been observed in the SLC DR and other machines. This instability, if occcurs, may be a limiting factor for the high-performance machines such as NLC DR. We review relevant experiments, theoretical models, and codes available for simulations.

Outline:

- **Steady State: Bunch Shape**
- **Experiments:**
  Energy Spread / Spectra / Relaxation oscillations
- **Models**
- **Simulations**
- **Impedance Issues**

Steady State:Bunch Shape

Approach:

Quasi-particles in a self-consistent potenial.
Haissinski steady-state solution of the V-F-Plank equation:

$$\rho(x,p)=\frac{1}{|N|}e^{-\left\{\frac{p^2}{2}+U(x|\rho)\right\}},\quad x=z/\sigma,\ p=-\delta/\delta_0,$$

$$\frac{\partial U}{\partial x}=x-\lambda\int dx'\rho(x')\,\sigma W[(x'-x)\sigma],$$

$$\lambda=\frac{N_b r_e}{2\pi R\alpha\gamma\delta^2},\quad \rho(x)=\int dp\,\rho(x,p),$$

$$W(s)=\int\frac{d\omega}{2\pi}Z(\omega)e^{-iks},\quad k=\frac{\omega}{c}.$$

Bunch Lengthening (PWD)

Experiment: R.Holtzapple,1996

Fig.1 Bunch Shape

Fig.2 σ(V)

Fig.3 σ(I) for the new/old vacuum chambers

Note:$\rho(x,p)=\rho(p)\ \rho(x)$ and bunch lengthening does not affect the energy spread.

K. Bane, 1995

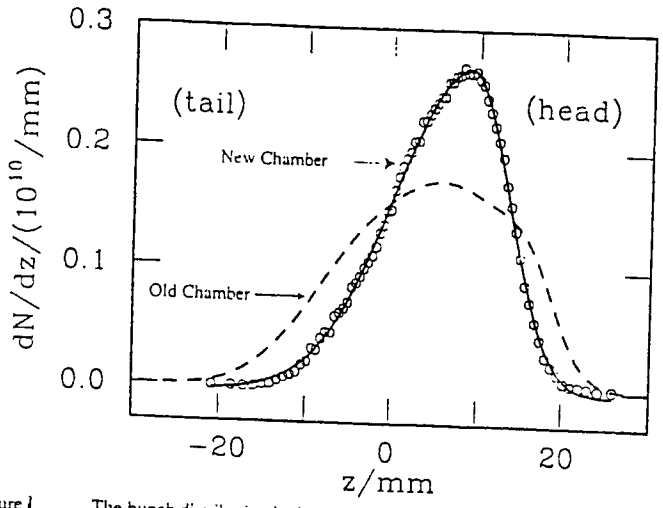

Figure 1 The bunch distribution in the electron damping ring at a current of 4.5×10^{10} particles per bunch for the old and new vacuum chambers [K. Bane et al. 1995].

R. Holtzapple. 1996

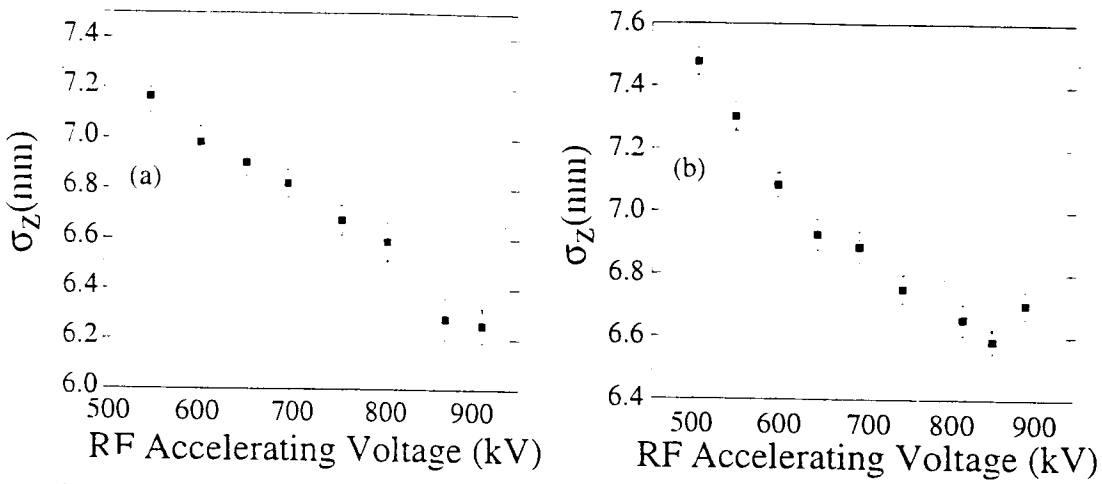

Figure 4. The bunch length as a function of RF accelerating voltage for the (a) positron and (b) electron damping rings.

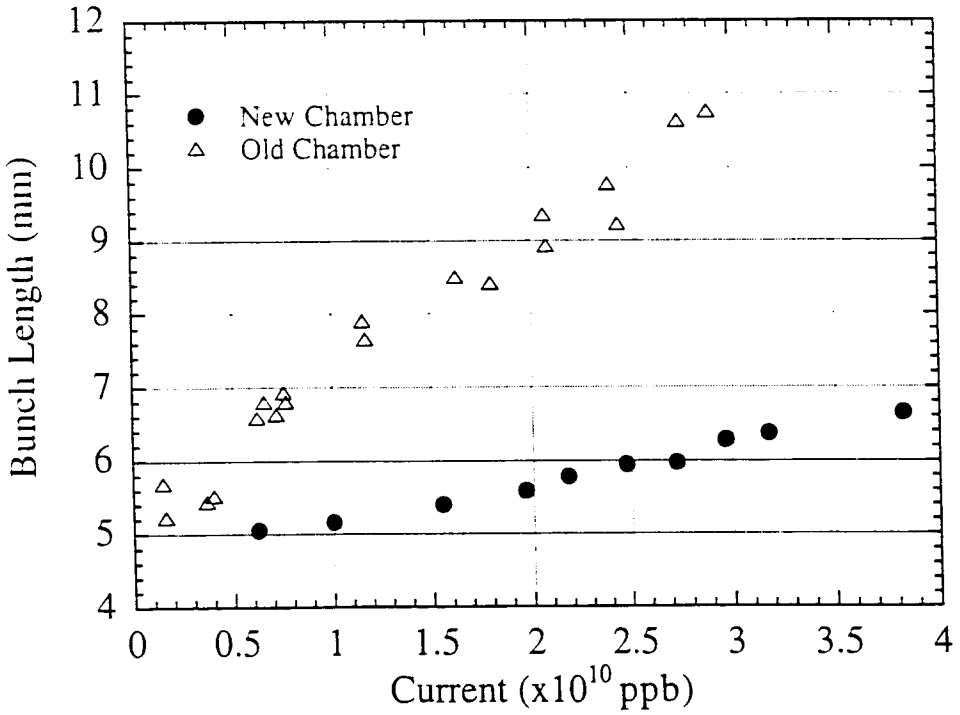

Figure 3. The bunch length as a function of current for the old vacuum chamber, measured with a wire scanner, and the new vacuum chamber, measure with the streak camera.

F: 2,3

Onset of Instability:

Fig. 4 δ(I), Holtzapple, 1996

Example:

Pure resistive wake: $Z(\omega) = R_s$, $W(s) = (4\pi R_s / Z_0)\,\delta(s)$

$$\frac{\partial U}{\partial x} = x - (4\pi R_s / Z_0)\,\lambda\,\rho(x)$$

With additional maximum of ρ (x) within a bunch, bunch splits *what may indicate onset of instability* .

This may be at $(4\pi R_s / Z_0)\left(\lambda / \sqrt{2\pi}\right) \geq 1$

what coincide with *Boussard* criterion for the threshold of MW instability:

$$\frac{I_{peak}}{2\pi (E/e)\,\alpha\delta^2}\left|\frac{Z}{n}\right| \geq 1,$$

where $\left|\frac{Z}{n}\right| = R/n_{max}$, and $n_{max} = R/\sigma$.

▼ (I, V) dependence of the I_{th}, Fig. 5.

▼ $\alpha = 0$ lattice: $\lambda \sim 1/\alpha$,
σ W changes with σ as $\sigma \frac{1}{\sqrt{\sigma}} \sim \sqrt{\sigma} \sim \alpha^{-1/4}$ (V = const),
and δ (I) grows with current faster than for larger
α although bunch lengthening may be suppressed for $\alpha < 0$.

▼ However, for pure inductive impedance $Z(\omega) = -iL\,\omega / c$,

$$\frac{\partial U}{\partial x} = x - \left(\frac{L}{\sigma}\right)\lambda\,\rho'(x)$$

criterion does not work, beam is stable. LER: up to 12 mA/bunch is stable

Holtzapple, 96

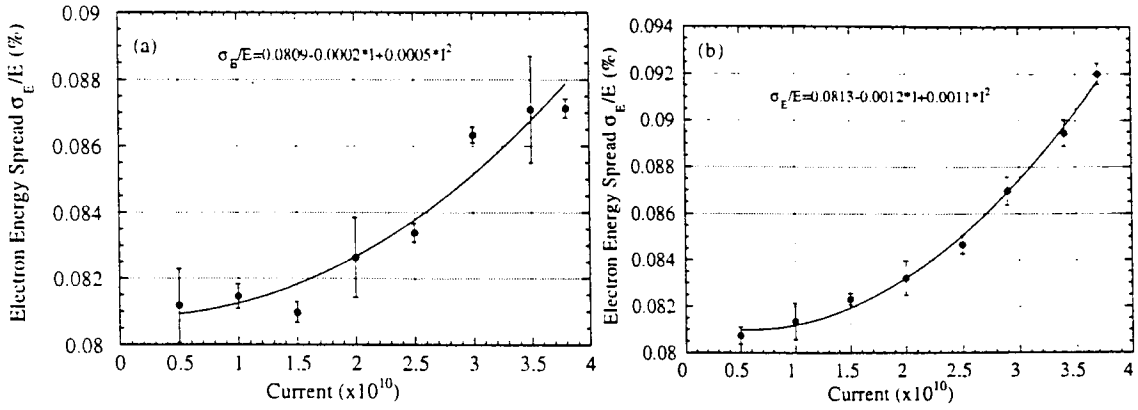

Figure 4 The energy spread of the electron damping ring as a function of current when the RF gap voltage was (a) 765 kV and (b) 940 kV.

F. 4 6

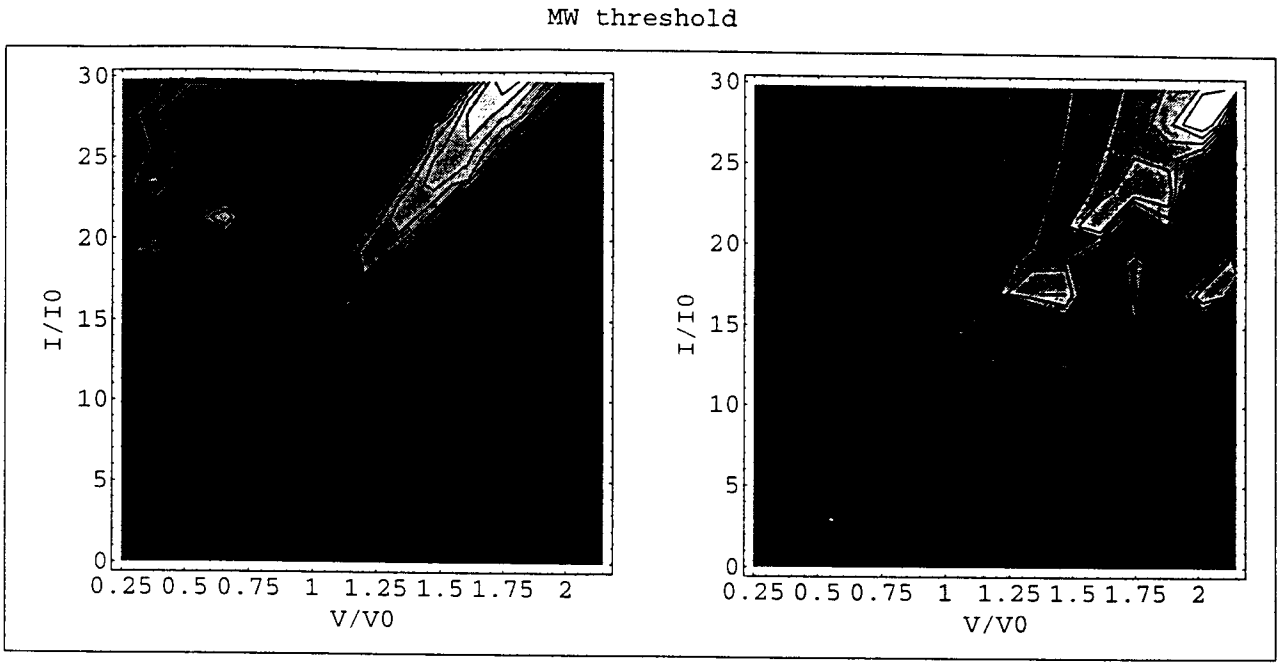

Contour of the parameter p(I,V) for sigma0/b=0.25 (left) and 0.5 (right). Beam is stable in the dark areas. BB Q=1 impedance.

A. Ogata et.al., TRISTAN

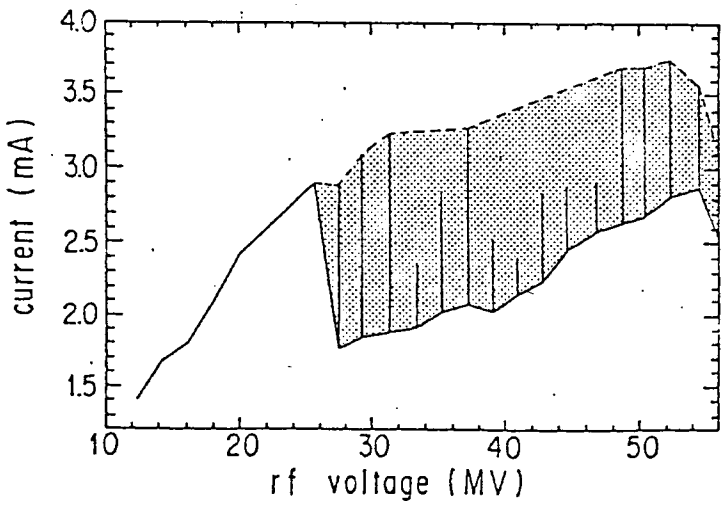

Fig. 1. An example of the inhibit band. $\nu_x = 36.605$, $\nu_y = 38.730$, $\xi_x = 0.95$, $\xi_y = 0.76$.

F.5

Beam Dynamics Above Threshold

- Increase of the energy spread
- Change of the bunch spectrum
- Saw-tooth oscillations of the side-band amplitude

These phenomena are quite common and has been observed in many laboratories.

Detail study: SLC DR, (P. Krejcik et al//B. Podobedov, R. Siemann), Fig. 6

Fig. 7, (Ogata et. al., TRISTAN)

Saw-tooth signal driven by a single RF mode was observed and studied at SPEAR, SSRL, (C. Limborg, J. Sebek), Figs. 8, 9

Saw-tooth oscillations in transverse motion (K. Harkey, et. al. APS, ANL), Fig. 10

B. Podobedov
B. Siemann

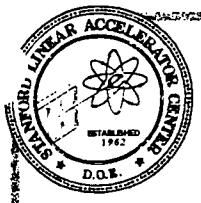

Typical Data for a Single Store

Spectrum Analyzer Data

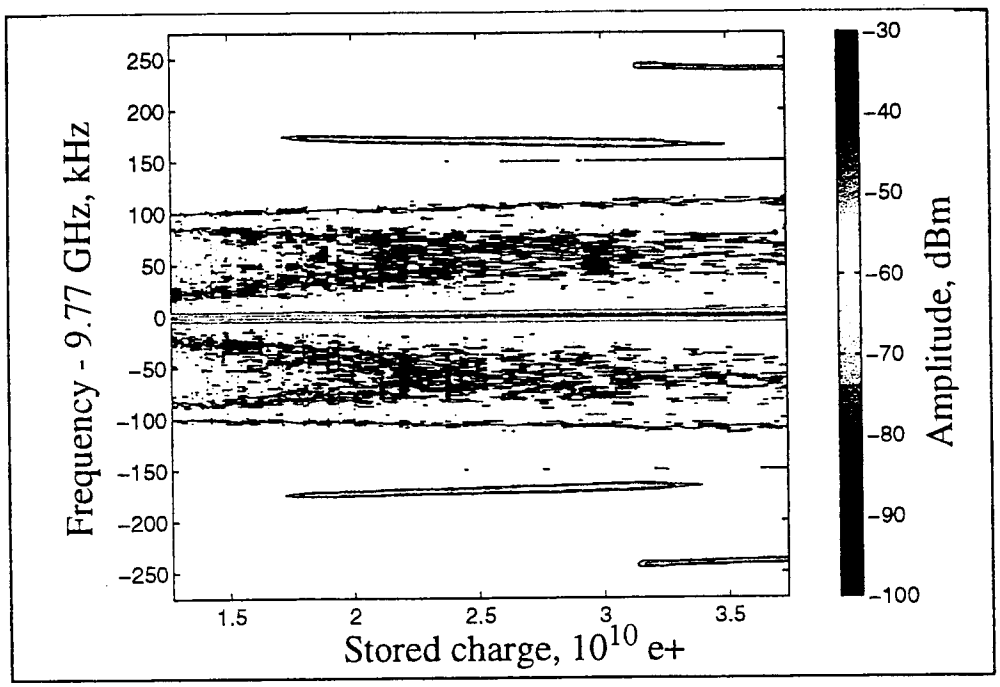

Scope Traces for Different Stored Charge

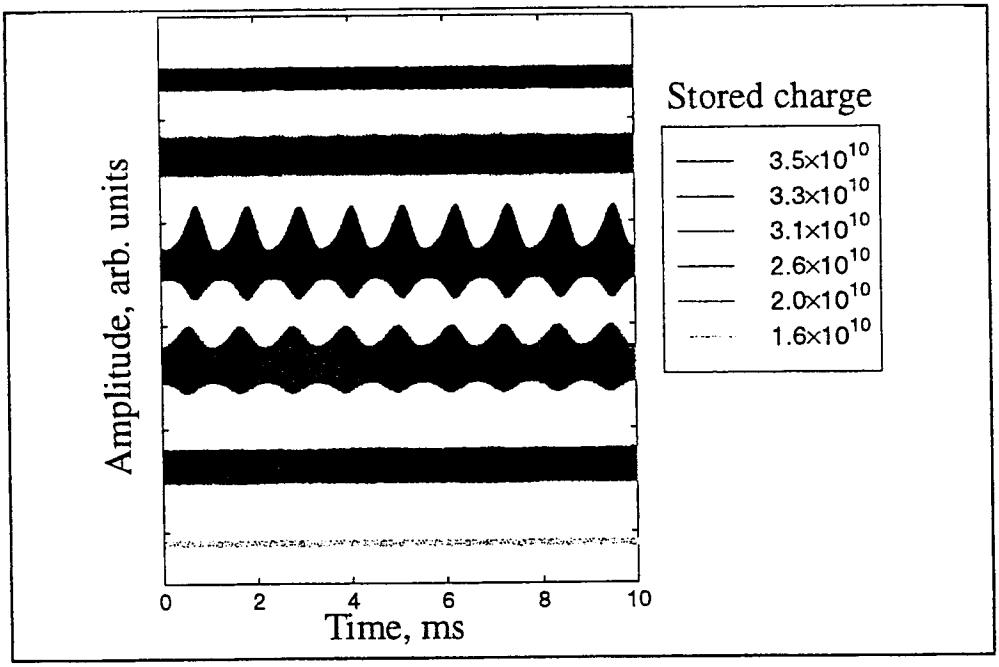

F.6

Ogata et al., 1988

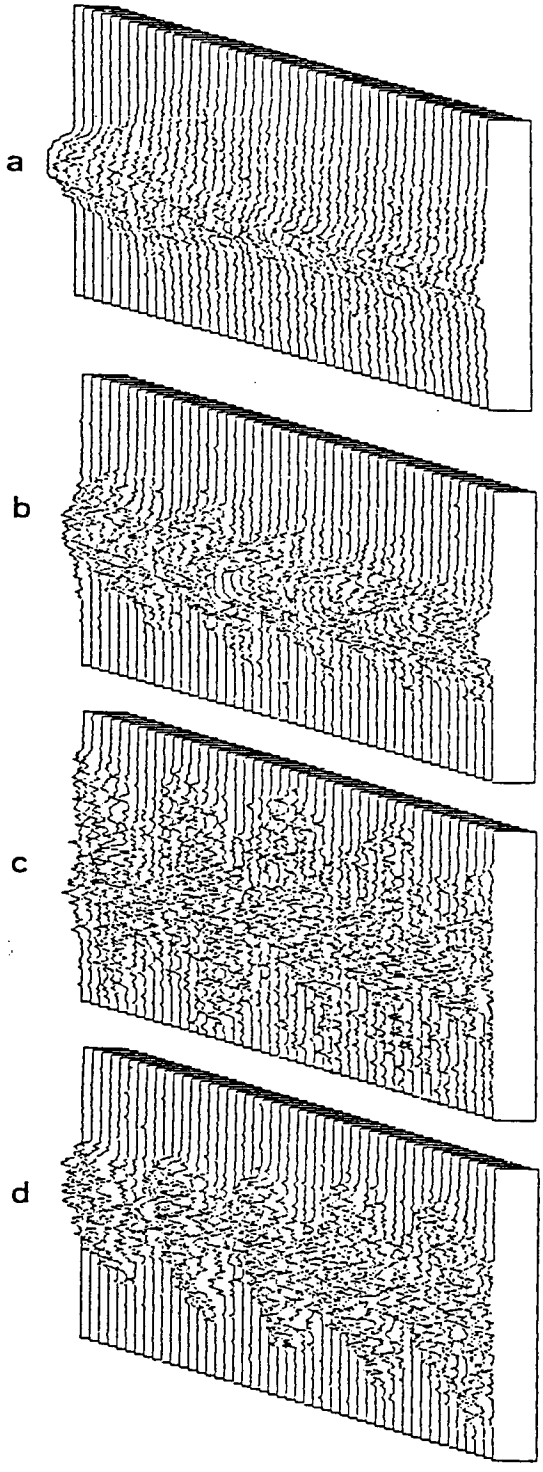

Fig. 4. Computer-processed streak pictures taken at the blowup. Vertical scale is 1.33nsec. Horizontal full scale is 9.6msec for (a) and 0.96msec for (b)-(d). Beam current is (a) 2.6mA, (b) 2.7mA, (c) 2.6mA, and (d) 2.0mA.

C. Limberg
J. Sebek

slow Fast

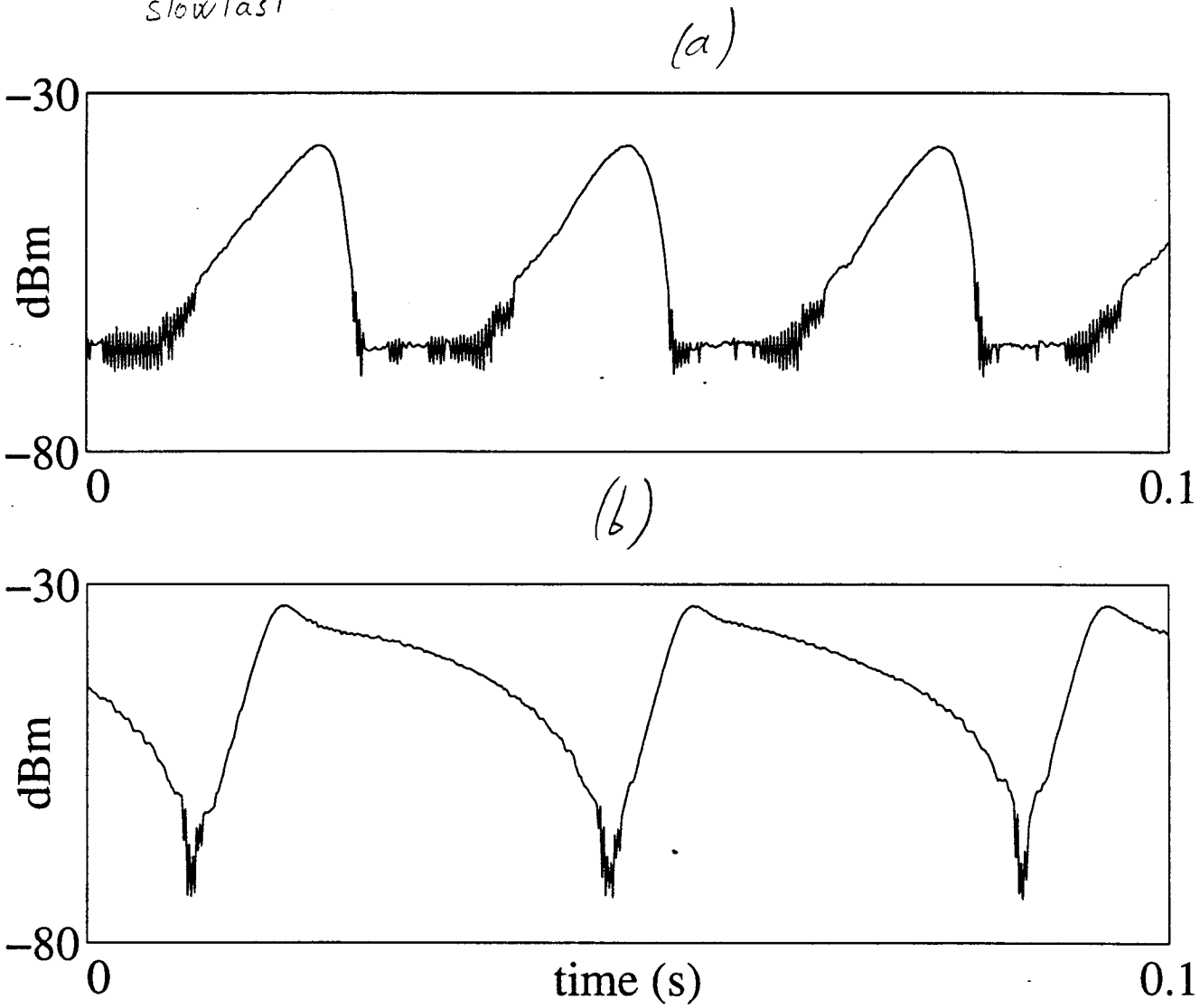

Figure (2)

F.8

C. Limborg
J. Sebek

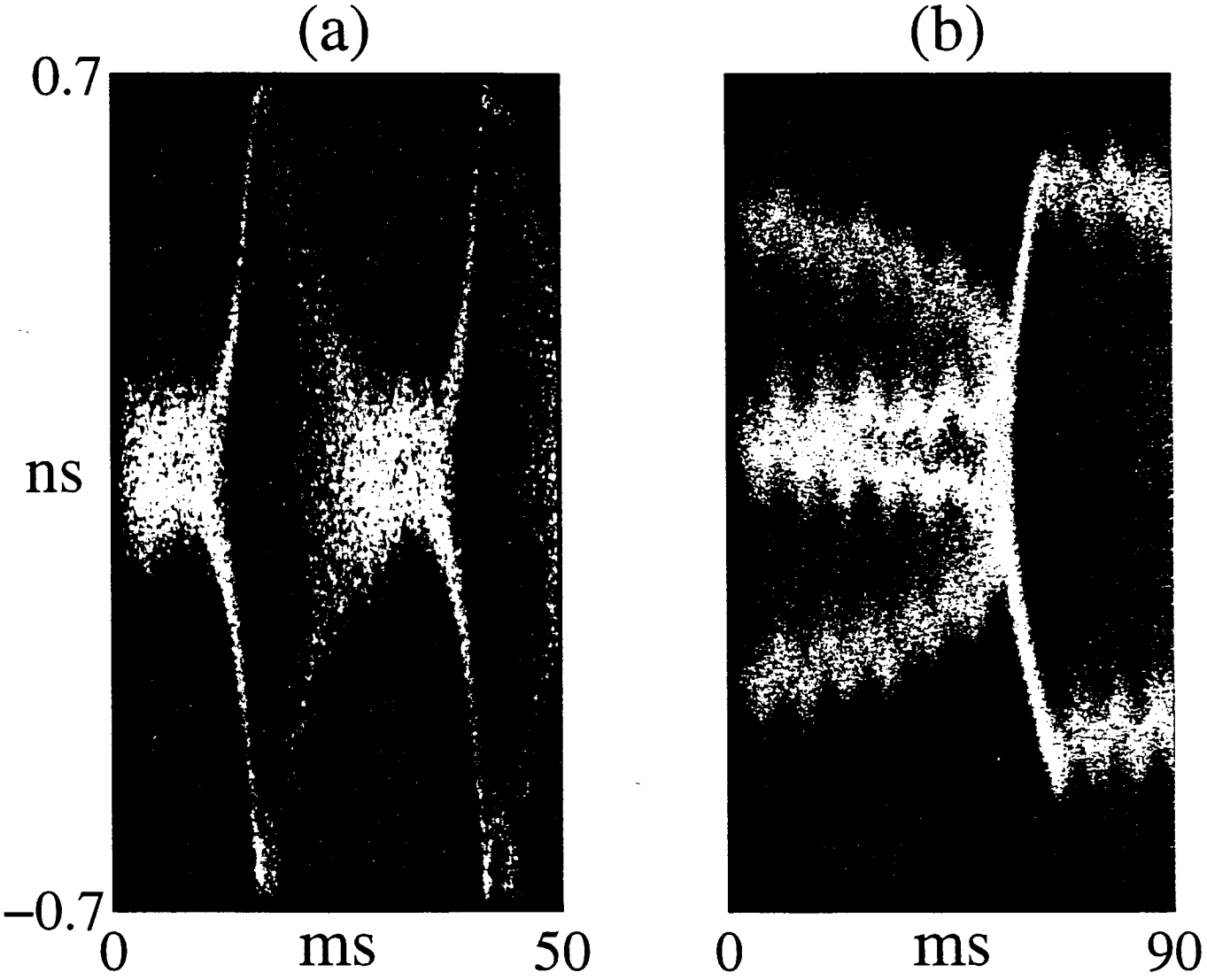

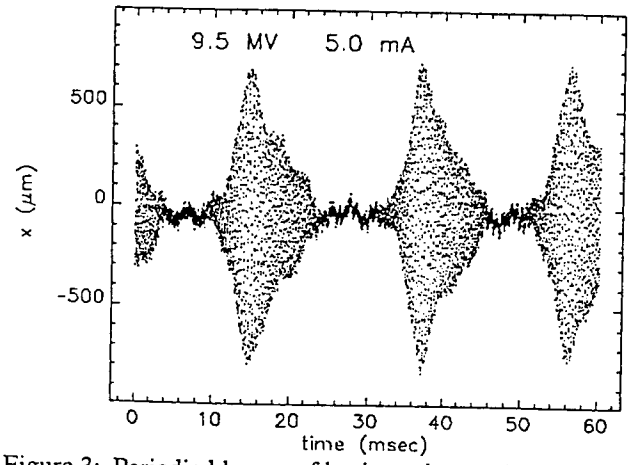

Figure 3: Periodic blowup of horizontal centroid motion.

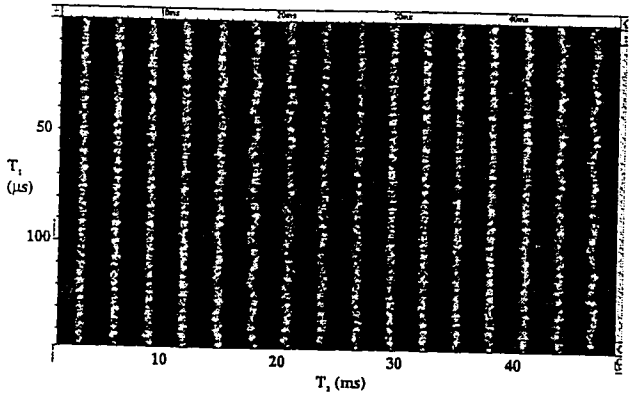

Figure 4: Horizontal oscillations observed using a streak camera in dual-sweep mode.

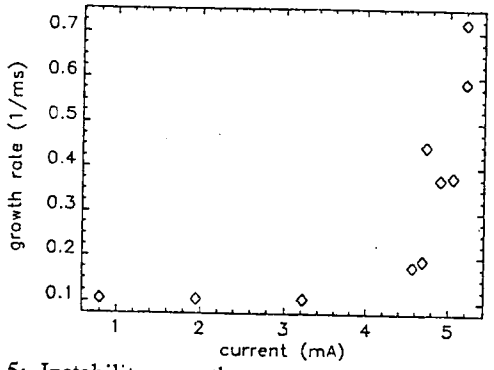

Figure 5: Instability growth rate vs. current.

Models of Instability

● MWI is the result of ineraction of many unstable modes decaying in the single-particle

motion and causing the turbulent heating of a bunch.

● Saw-tooth instability (STI) can be considered as the onset of the MW instability.

● The STI can usually be explained by excitation of a single or

only few modes. This still leaves open several possible scenarios.

Extreme scenarios:

● ***The overshoot phenomena (generic description)*** ("strong MWI")

★ **An unstable mode growth causing PWD what results in the mode**

saturation.

★ **The unstable mode decays leading to the bunch heating.**

★ **The SR damping restores initial distribution and the cycle repeats. Fig. 11**

● ***Dyachkov-Baartman model***

requires strong PWD leading to the two-minima self-consistent potential,

populated by quantum fluctuations of the SR.

These models require substantial perturbation of the distribution function. They may correspond to a "strong" MWI and be inconsistent with experiments

at the threshold of the instability where the coherent signal is caused

by only small percentage of particles.

C. Limbos
J. Sebek

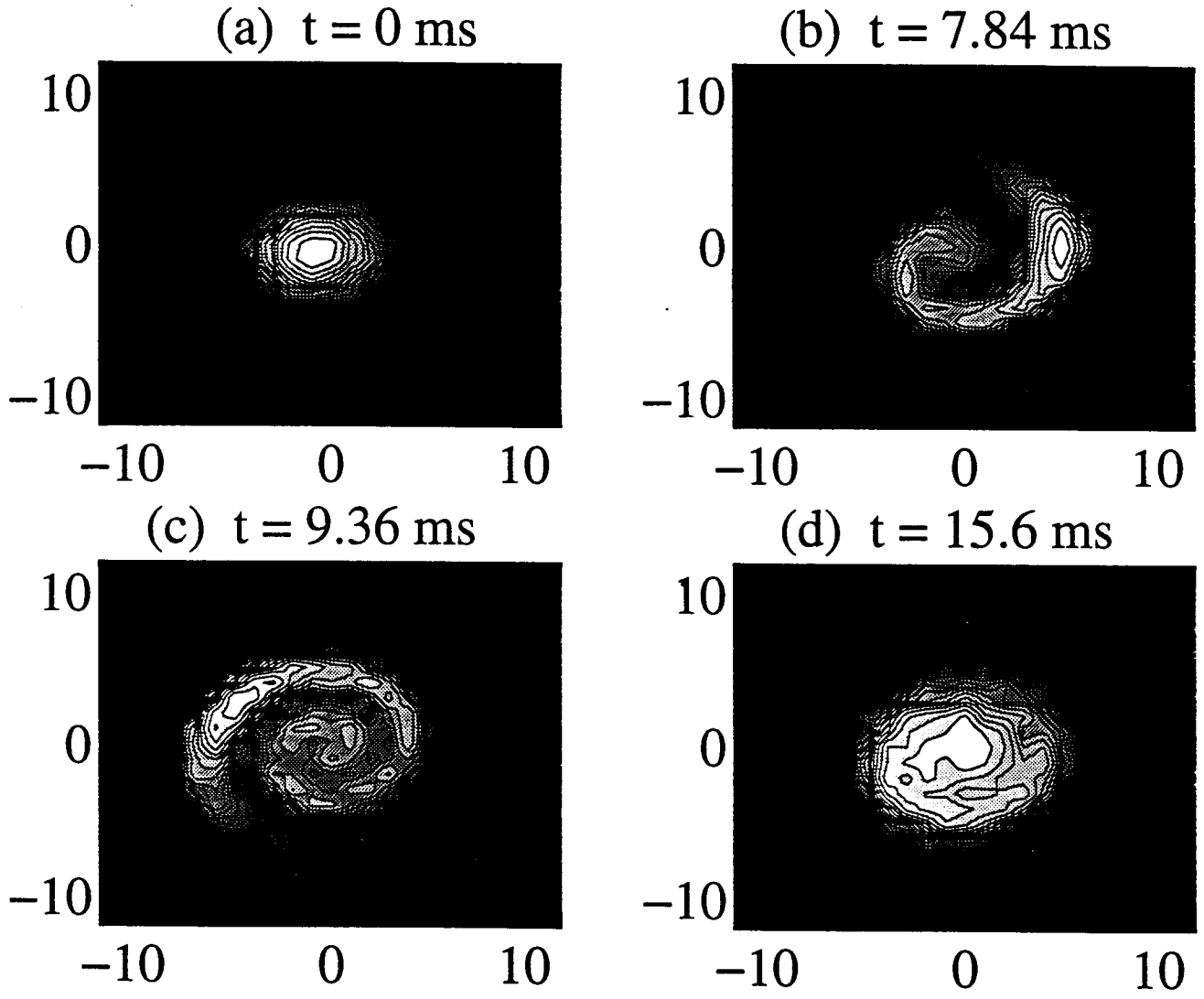

the opposite extreme case,

Mode interaction.

● *A single unstable azimuthal mode:*

✸ The instability is caused by the anharmonicity of the particle trajectory, related to $U(x) \sim \alpha x^3$ (Oide)

✸ The mode as an external periodic perturbation trapes partilces with amplitudes $J \sim J_s$ in an analogy with a nonlinear oscillator, Fig. 12

✸ Traped particles produce a periodic signal with frequency $m\omega_s(J_s)$ and introduce (z,p) correlations changing the energy spread δ.

✸ The growing mode produces additional diffusion modifying distribution function and self-consistent potential (O'Neil//Y.Chin-K. Yokoya)

$$\frac{\partial \rho(J,t)}{\partial t} = \frac{\partial}{\partial J}\left[\left(D\frac{J}{\omega(J)} + D_{ind}\right)\frac{\partial \rho}{\partial J} + J\right],$$

$$D_{ind} = \frac{2m\Gamma}{[\omega(J)-\omega(J_s)]^2+\Gamma^2}\,|V_m|^2.$$

✸ As a result, the mode may saturate at a finite amplitude leading to a new steady-state in rotating frame of the separatrix (Shonfield//Meller//S.H.)

✸ In the lab frame the steady-state distribution is a superposition of azimuthal harmonics.

✸ The zero harmonics is substantially different from Haissinski distribution only in the vicinity $J \sim J_s$, changing $\partial\rho / \partial J \to 0$ what explains the mode saturation, Fig. 13

✸ The resonance Hamiltonian in the rotating frame

$$H(J,\phi) = \frac{\omega'(J)}{2} J^2 + V \sin(\phi)$$

at large J has two FP at $\phi=0$ and $\phi=\pi$. Growth of the amplitude of unstable mode may change the sign of ω', leading to a saw-tooth behavior.

✸ Essential features of the beam dynamics has been demonstrated in the Byrd-Zimmermannexperiment.

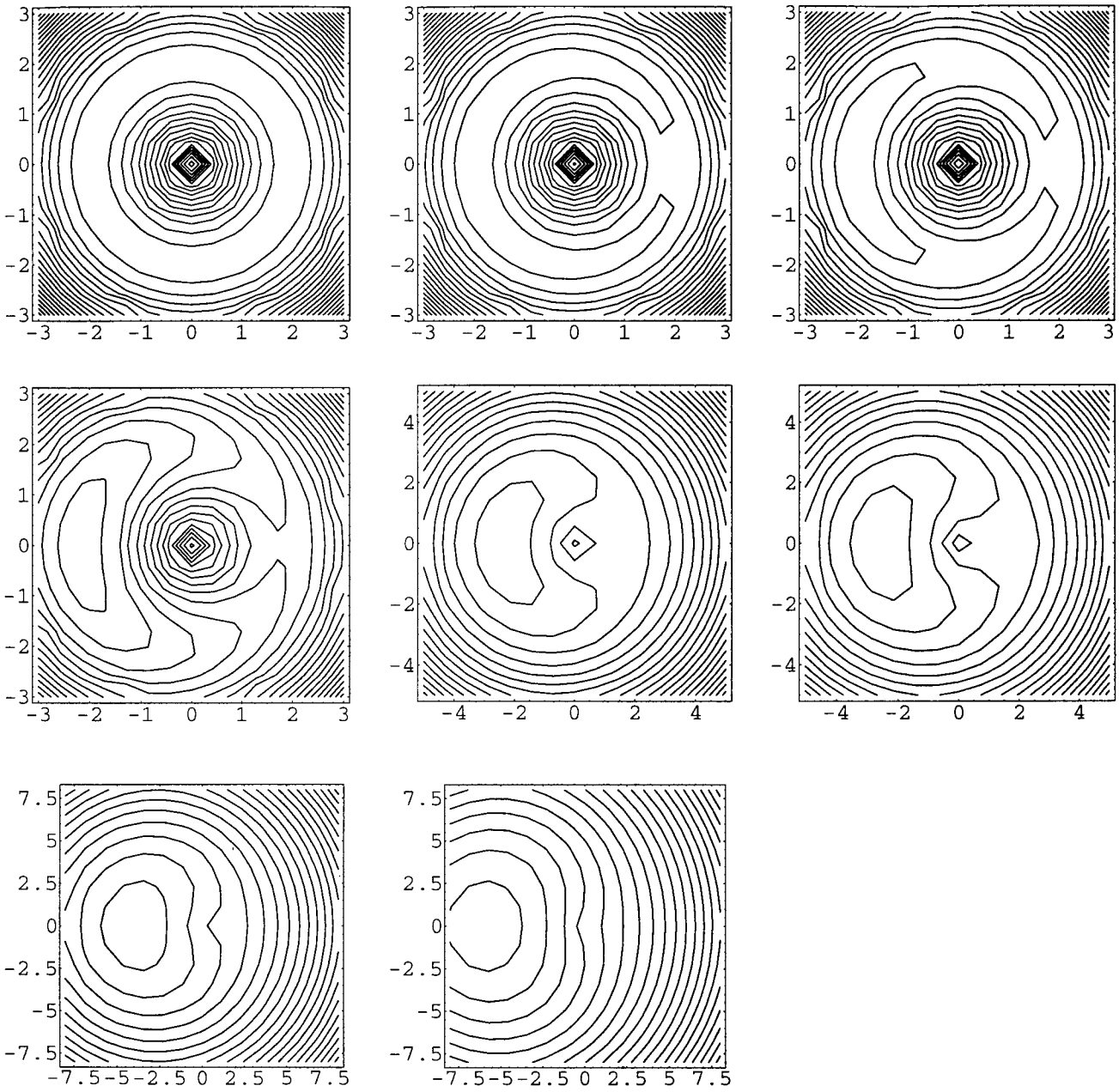
3 2 1 0 -1 -2 -3
-3 -2 -1 0 1 2 3
4 2 0 -2 -4
-4 -2 0 2 4
7.5 5 2.5 0 -2.5 -5 -7.5
-7.5 -5 -2.5 0 2.5 5 7.5

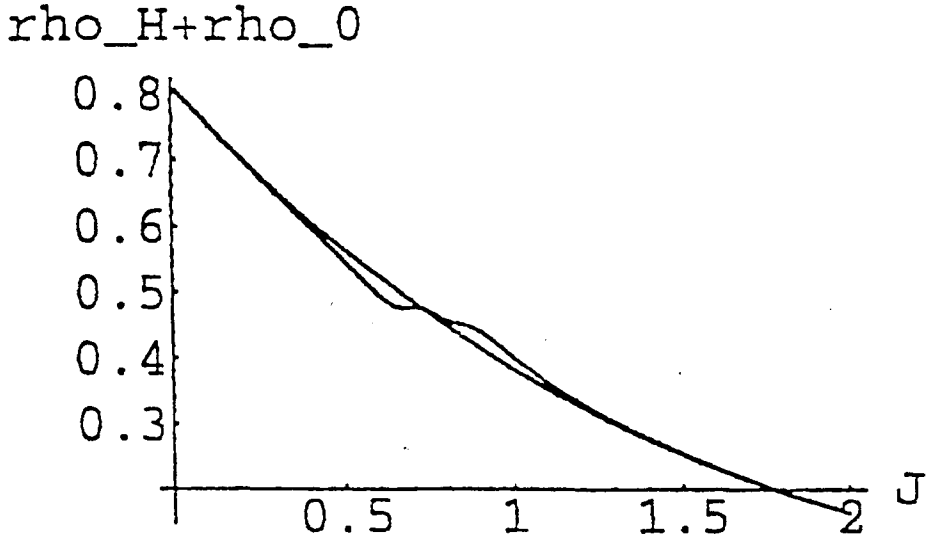

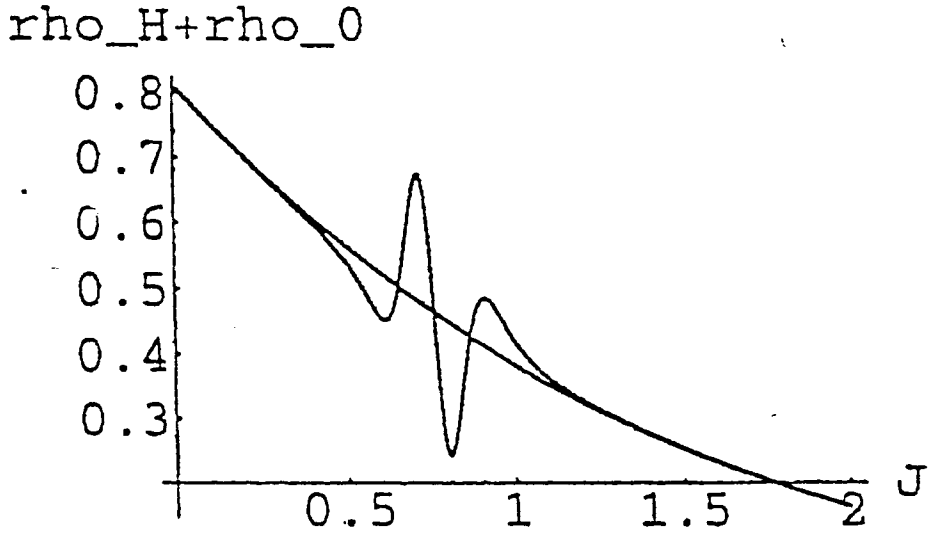

Distribution function (m = 0) pertubed by dipole (m = 1, above) and quadrupole (m=2)

● ***Interaction of unstable modes or unstable/stable modes***

may lead to periodic unharmonic modulation of their amplitudes.

✱ Interaction can be the interaction of different azimuthal modes or radial modes of the same azimuthal mode. ("weak MWI")

✱ Simulation show that unstable mode interacting with a stable mode may saturates while stable mode become unstable, Figs. 15,16,17

This may explain the "jumps" of presence of the sidebands in the bunch spectrum.

✱ For $\omega(J)$ having minimum, as in the case of R+L impedance, there are two

rad-mode with the same frequency, which may strongly perturbe each other.

The lowest current, at which $\omega'(J)=0$ at least for some amplitude, may be taken as the threshold current of a "weak" MW instability (Oide).

✱ Similar results has been obtained in different technique by Breizman et. al.

● ***The compromise model:*** "Dynamic Baartman-Djachkov"

is given by the model were particles are traped in the separatrices of unstable modes.

The population and the size of the separatrices are determined by the dynamics of the instability in a self-consistent way: drift of particles from one separatrix to another changes ρ_0 and the growth rate of instability. Together with SR damping this may lead to periodic anharmonic oscillations (Limborg-Sebek//Mosnier).

Qualitative Scenario of the Instability

Below threshold: H=H_H; $\rho = \rho_H \sim e^{-H_H}$.

Introduce perturbation: $H_H(J) \rightarrow H = H_H(J)+V(J)\,\mathrm{Cos}[\phi-\Omega t]$.

In the variables of rotating frame:

$\alpha=\phi-\Omega t$, I=J, $H(I,\alpha)=H_H(I)-\Omega I + V(I,t)\,\mathrm{Cos}[\alpha]$

V-Fk-Pl. equation $\frac{\partial \rho}{\partial t}+\{H,\rho\}=\gamma_d[\frac{J}{\omega(J)}\ \frac{\partial \rho}{\partial t}+J\rho]$

for ***small V*** is dominated by the RHS, $\rho=(1/N)\, e^{-[H_H+\sigma(I,\alpha,t)]}$

where, for $V(I,t)=\epsilon(I)\, e^{\Gamma t}$, in linear approximation,

$\sigma=\frac{V(I,t)\,\omega_H}{2(\omega_H-\Omega+i\Gamma)}\, e^{i\alpha}+c.c.$

Condition of the self-consistency, $u(J,\phi,t)=\lambda\int dJ' d\phi'\, \rho(J',\phi',t)\, K(J,\phi,J',\phi')$

in the linear approximation gives the usual d.eq.:

$V(J,t)=2\pi\lambda\int dJ' \frac{K_{11}(J,J')\,V(J',t)}{\omega_H(J')-\Omega+i\Gamma}$.

Large V:

Main effect-particle traping, $\rho \sim e^{-[H_H(I)-\Omega I + V(I,t)\,\mathrm{Cos}\,\alpha]}$.

Approximate $\rho=\rho_1+\rho_2$, $\int dI\, d\alpha\, \rho_1=N_1$, $\int dI\, d\alpha\, \rho_2=N_2$, $N_1+N_2=1$,

as two -macro partciles (A. Chao) located at the FP: $(J_1,0)$, (J_2,π).

Condition of self-consistency in the approxiamtion for trajectories of free particles

$x(I,\alpha)=\sqrt{(\frac{2I}{\omega})}\,\mathrm{Cos}\,\alpha$, and $Z(\omega)=R_s$ gives

$V(J)=\frac{4\pi R_s}{Z_0}[-N_1\sqrt{1-J_1/J}\ \theta(J-J_1)+N_2\sqrt{1-J_2/J}\ \theta(J-J_2)]$.

Diffusion changes population of the FP separatrices N_1, N_2 and the sign of V.

The stable/unstable FP interchange, and damping brings everything back where it started.

Mode Coupling

$$\rho(J,\phi,s) = \rho_H(J) + \sum_n \rho_n(J) e^{in\phi}, \tag{1}$$

$$\rho_n(J,s) = \rho'_H(J) \sum_\nu b_\nu X_\nu(J) e^{-i(\omega_H - \bar{\omega})s}. \tag{2}$$

X_ν are eigen vectors of the matrix of linear problem:

$$\int dJ' M_m(J,J') X_\nu(J') = -\nu X_\nu(J). \tag{3}$$

The radial amplitudes satisfy equations

$$\dot{b}_\nu + (i\nu + \gamma_d) b_\nu + i \sum_{\mu,\sigma} C^\nu_{\mu,\sigma} a_\mu b^*_\sigma + i \sum_\sigma d_{\nu,\sigma} b_\sigma = 0, \tag{4}$$

$$\dot{d}_{\nu\sigma} + \gamma_0 d_{\nu\sigma} = -i(\nu'^* - \sigma') P^{\nu,\sigma}_{\nu',\sigma'} b^*_{\nu'} b_{\sigma'}, \tag{5}$$

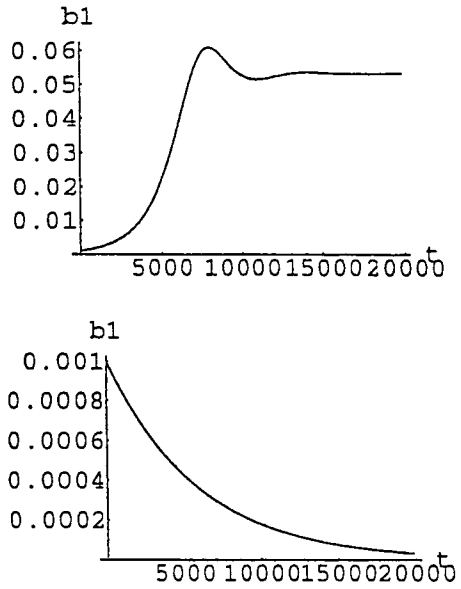

Above : Limiting Cycle, gamdip = 0,

Below : Stability, gamdip = 8. 10 ^ (-4)

Fig. 14

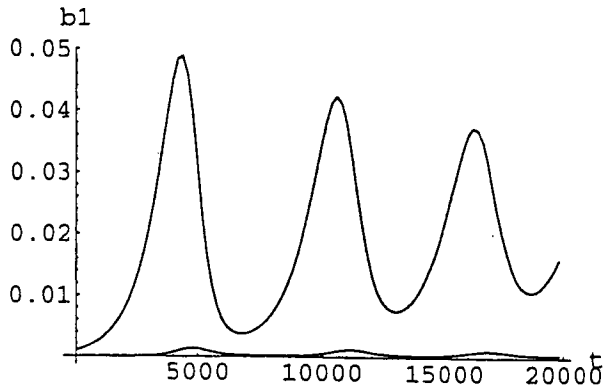

Out[65]= - Graphics -

**Amplitude of linearly unstable dipole mode (above)
and dynamic decrement (below) due to coupling to rho_ 0.
When tha latter is larger than linear increment (0.0019)
growth reverses sign .**

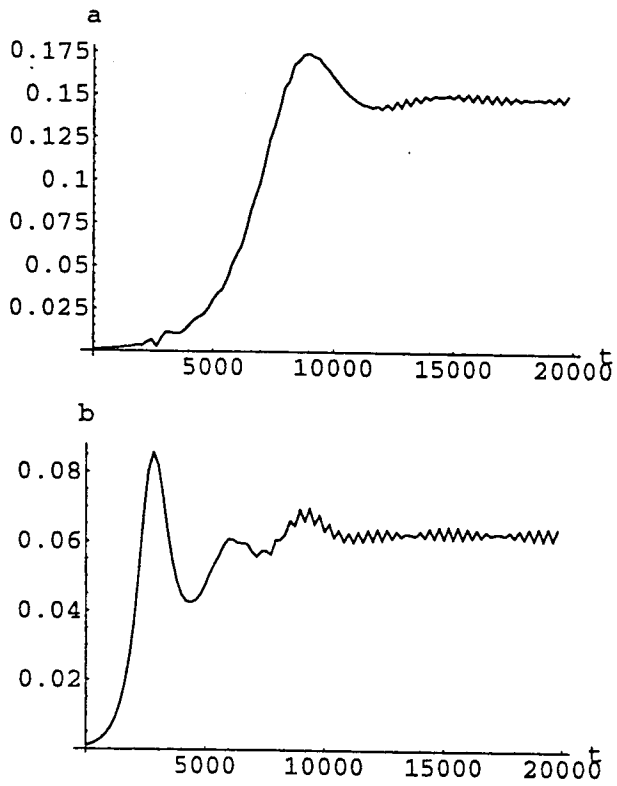

Out[58]= - Graphics -

lambda = 6.88447 alpha = 0.9 mu = 1.5

gam0 = 0.001 gamdip = 0.0001 gamquad = 0.0001

Dipole + Quadrupole modes, both linearly unstable. Stabilization is due to nonlinear interaction.

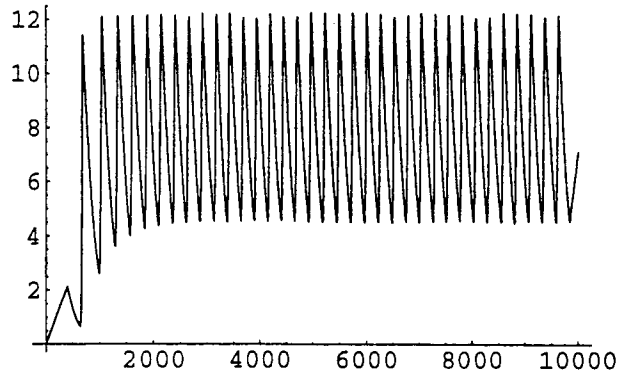

lambda=2.4 alph=0.5 om'=0. om2p=0.1 jbar=0.5

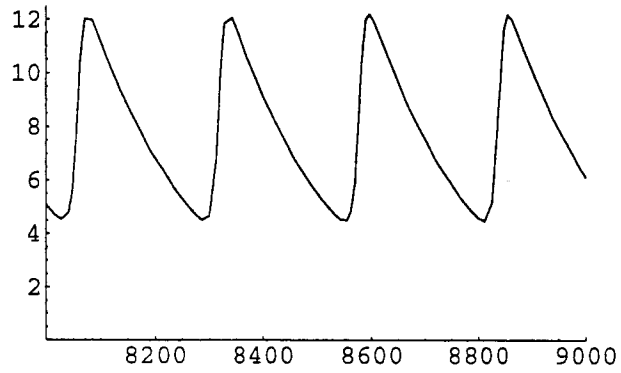

lambda=2.4 alph=0.5 om'=0. om2p=0.1 jbar=0.5

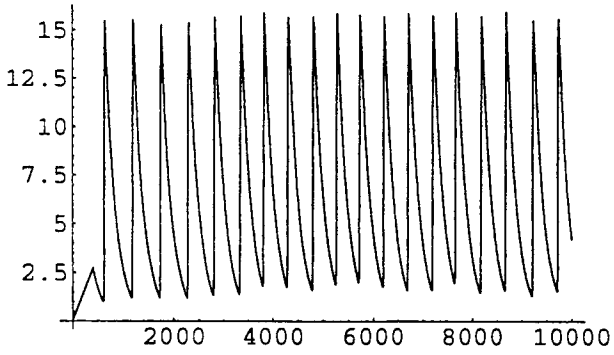

lambda=2.6 alph=0.5 om'=0. om2p=0.1 jbar=0.5

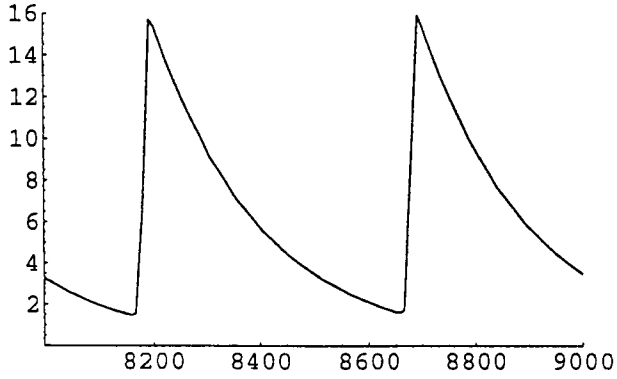

Simulations

Three way to approach the problem:

1. Tracking (K. Bane//Saabi,TRISIM)
2. Numerical solution of the linearized Vlasov equation (Oide-Yokoya//Mosnier)
3. Direct numerical solution of the V-Fk-Plank equation (A. Novokhatski//R. Warnock)

Tracking:

K. Bane: Fig. 18
TRISIM for PEP-II, Fig. 19

Linearized Vlasov:

Oide,

1. Analysis of the eigen values of the box matrix (m,J),
2. Includes PWD,
3. Mode crossing ,
4. Dependence of $\delta(I)$ is from setting I to $I_{th}(\delta)$,
5. Fig. 20 , growth time τ, Im $\mu=1/(\tau\omega_s)$,

Compare with Boussard:

PEP-II: τ_d=20 ms, Im $\mu\sim10^{-3}$, kR~1
NLC DR: Im $\mu\sim1.2\ 10^{-2}$, kR~2.5

6. Fig. 21 L+R stabilization

K. Bane

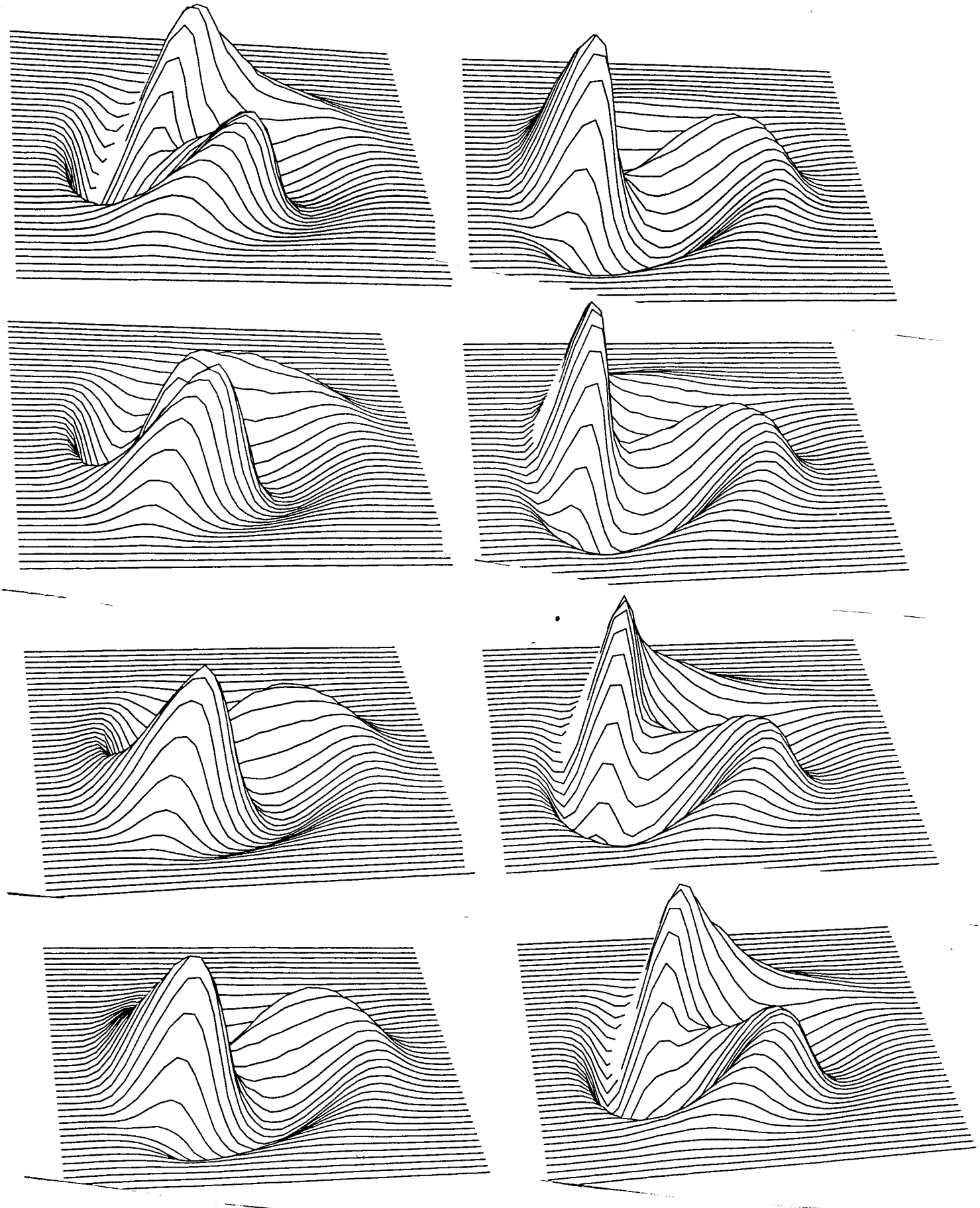

F.18

INPUT FILE NAME lersum (part 1) RUN DATE 22/ 5/ 96 TIME 10. 37. 19

Distributions are approximated by linear interpolation (8.333 ps step)
Longitudinal wake switched ON – Transverse wake switched OFF

Number of particles	1000	Damping time (s)	0.03	Beam energy (GeV)	3.109
Number of turns	20000	Energy spread (MeV)	2.51	Radiation loss (MeV)	1.14

Bunch current (mA)	1.81	Betatron tune	34.64
Total RF Voltage (MV)	6.05	Synchrotron tune	0.037

Equilibrium values (averaged over 200 turns)

Bunch center (ps)	15.383	Bunch length (ps)	27.537	Bunch width (mm)	0.185
Mean energy (MeV)	−0.577	Energy spread (MeV)	2.107	Total losses (MeV)	0.88

Total CPU time (s) 293.481 Time for wake calculation (s) 56.886

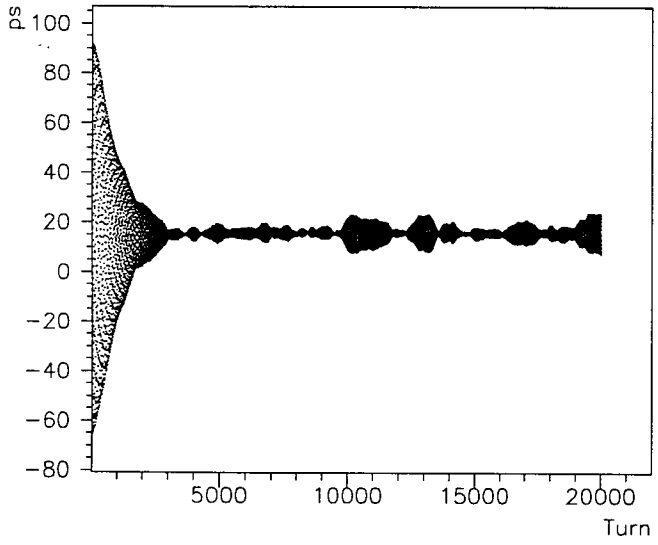

Longitudinal center of charge

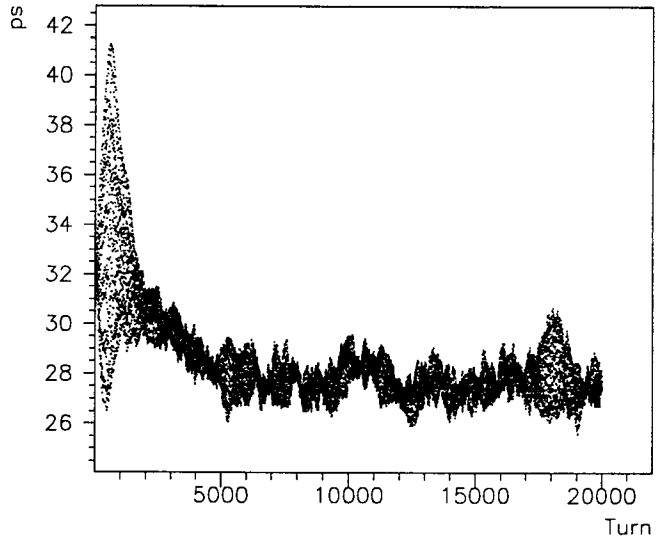

RMS bunch length

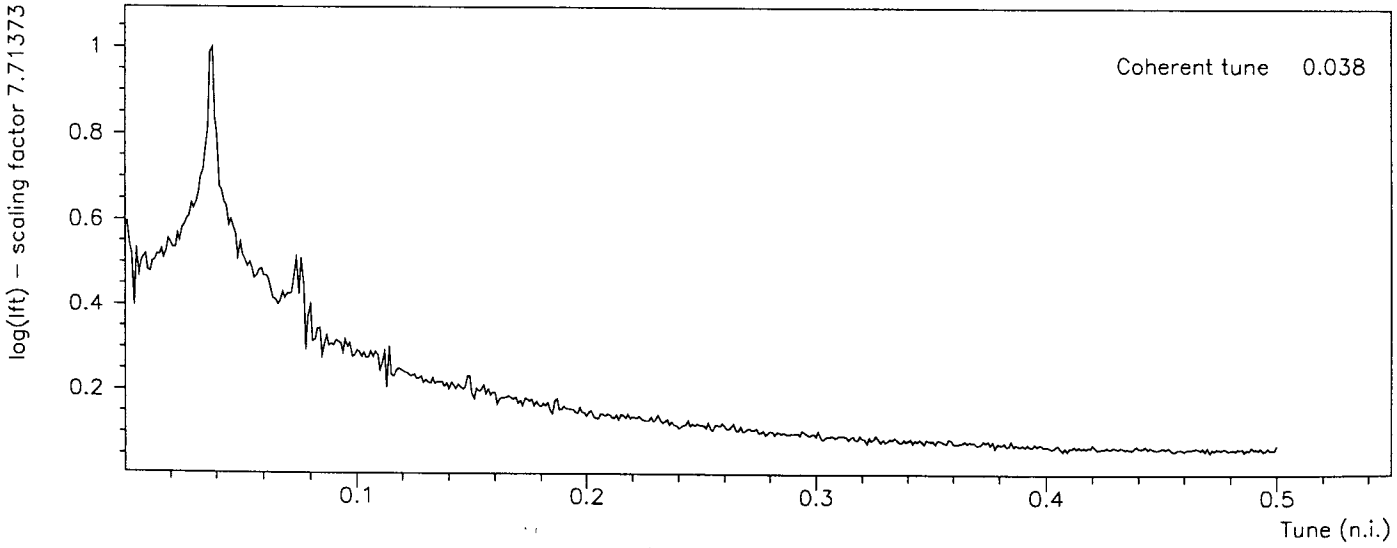

Longitudinal oscillation modes

TRISIM – SIMULATION OF COHERENT INSTABILITIES AT LEP

dE vs time–ps

RUN DATE 10/ 2/ 99 TIME 16. 27. 18

Distributions are approximated by linear interpolation in steps of 7.5 ps

Longitudinal wake switched ON

Transverse wake switched OFF

Number of particles 1000

Current per bunch (mA) 1000

BUNCH CONFIGURATION AT TURNS 9932 9940 9948 9956

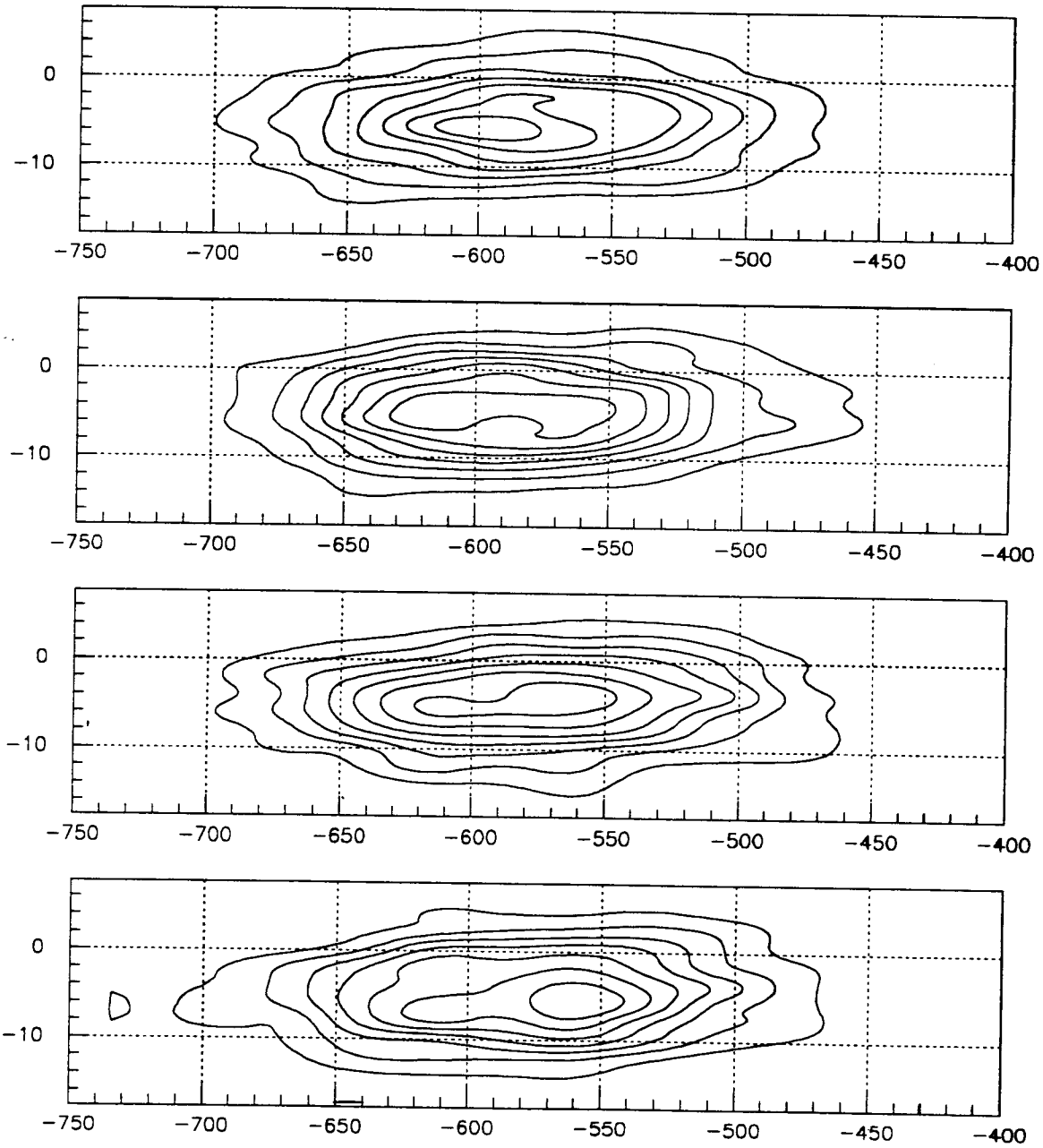

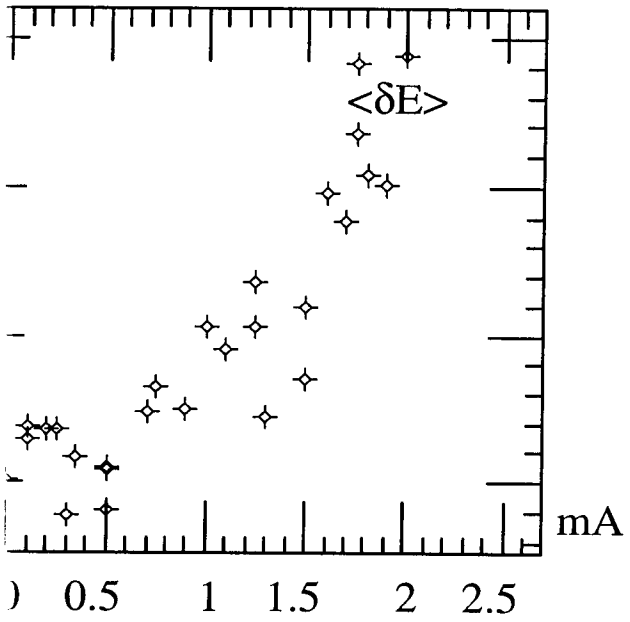
<δE>
mA
0.5
1
1.5
2
2.5

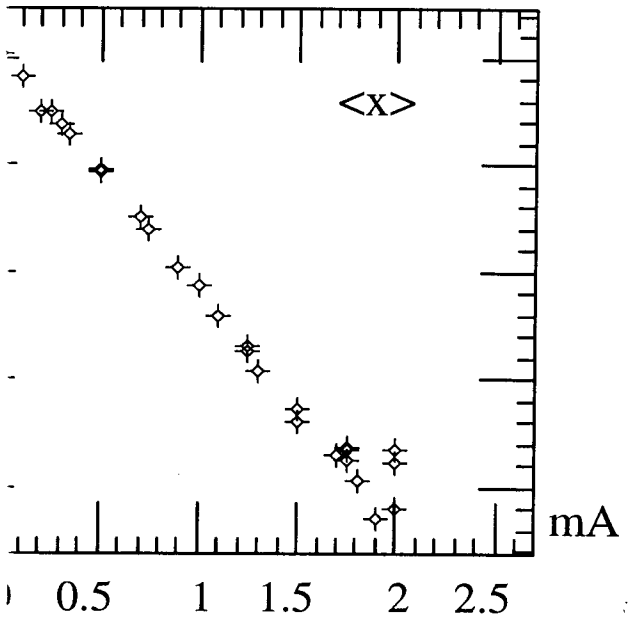
<x>
mA
0.5
1
1.5
2
2.5

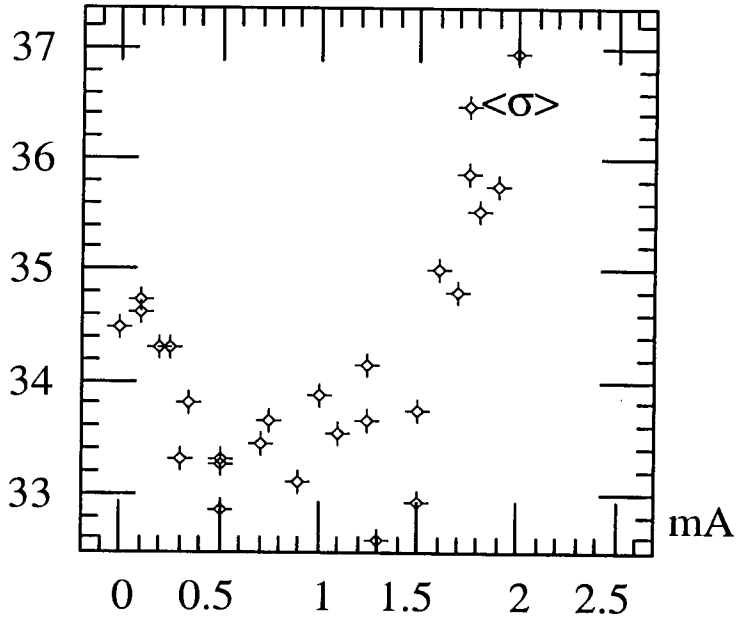
<σ>
37
36
35
34
33
mA
0
0.5
1
1.5
2
2.5

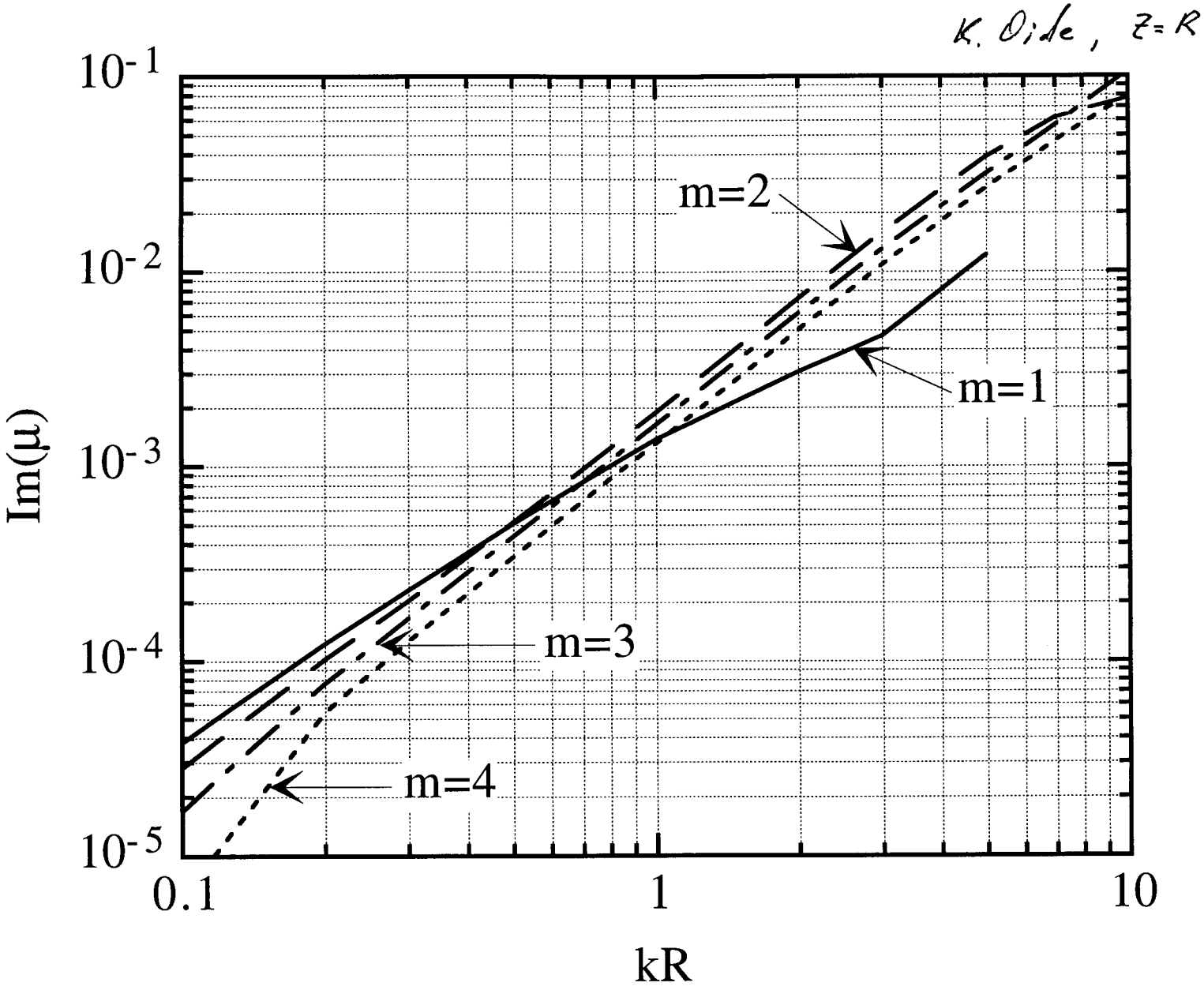

Fig. 20

K. Oide

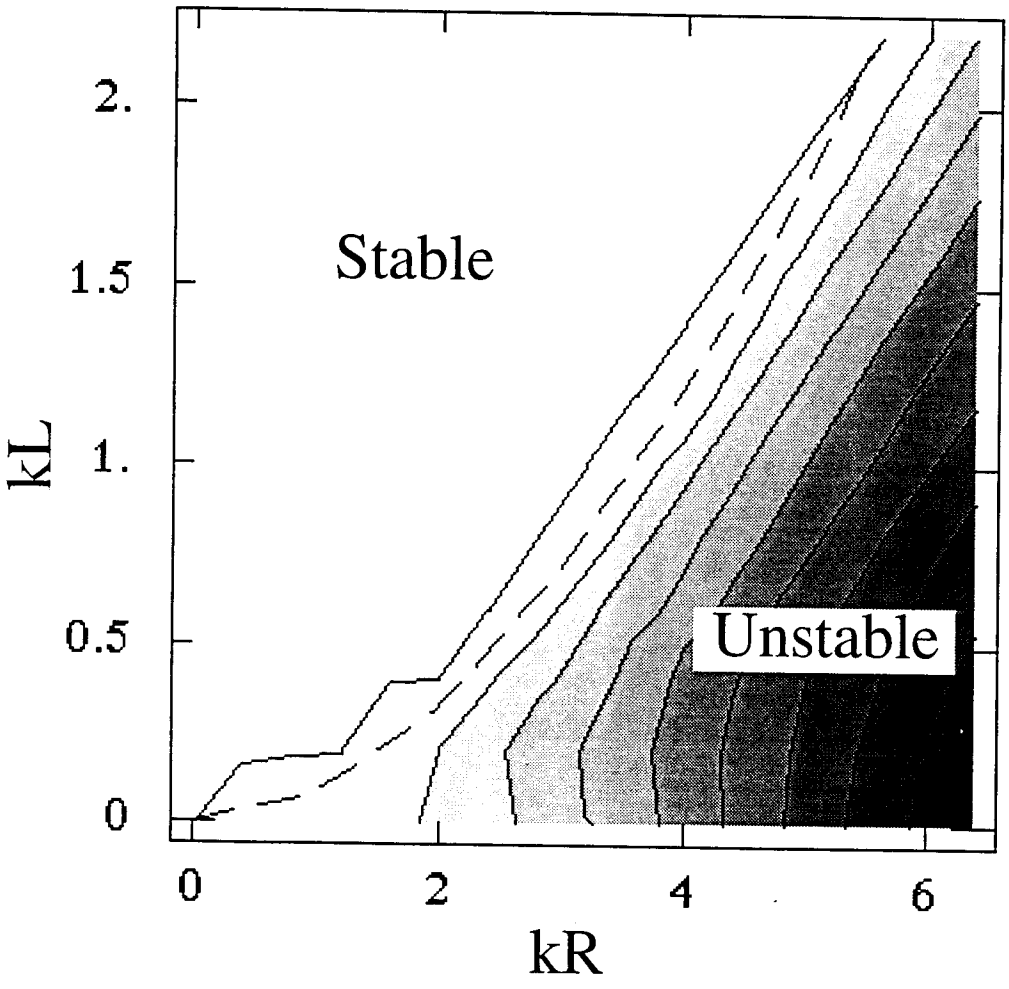

Fig. 21

Mosnier, *simulation of the BB resonator*

$\omega_r \sigma / c >> 1$, *m* – coupling comes first,

$\omega_r \sigma / c << 1$, rad – coupling comes first.

In the second case, large dipole and quad oscillations. Bunch may

Threshold current has minimum at $\omega_r \sigma / c$=1.25, see Fig. 22

Harmonic cavities increase I_{th} reducing peak current but reduce

Fokker-PlankSolver

Fig. 23, Fig. 24 (Novokhatski),
Fig. 25 (R. Warnock)

Note: only small ripples contrary to D-B model

A. Novokhatski

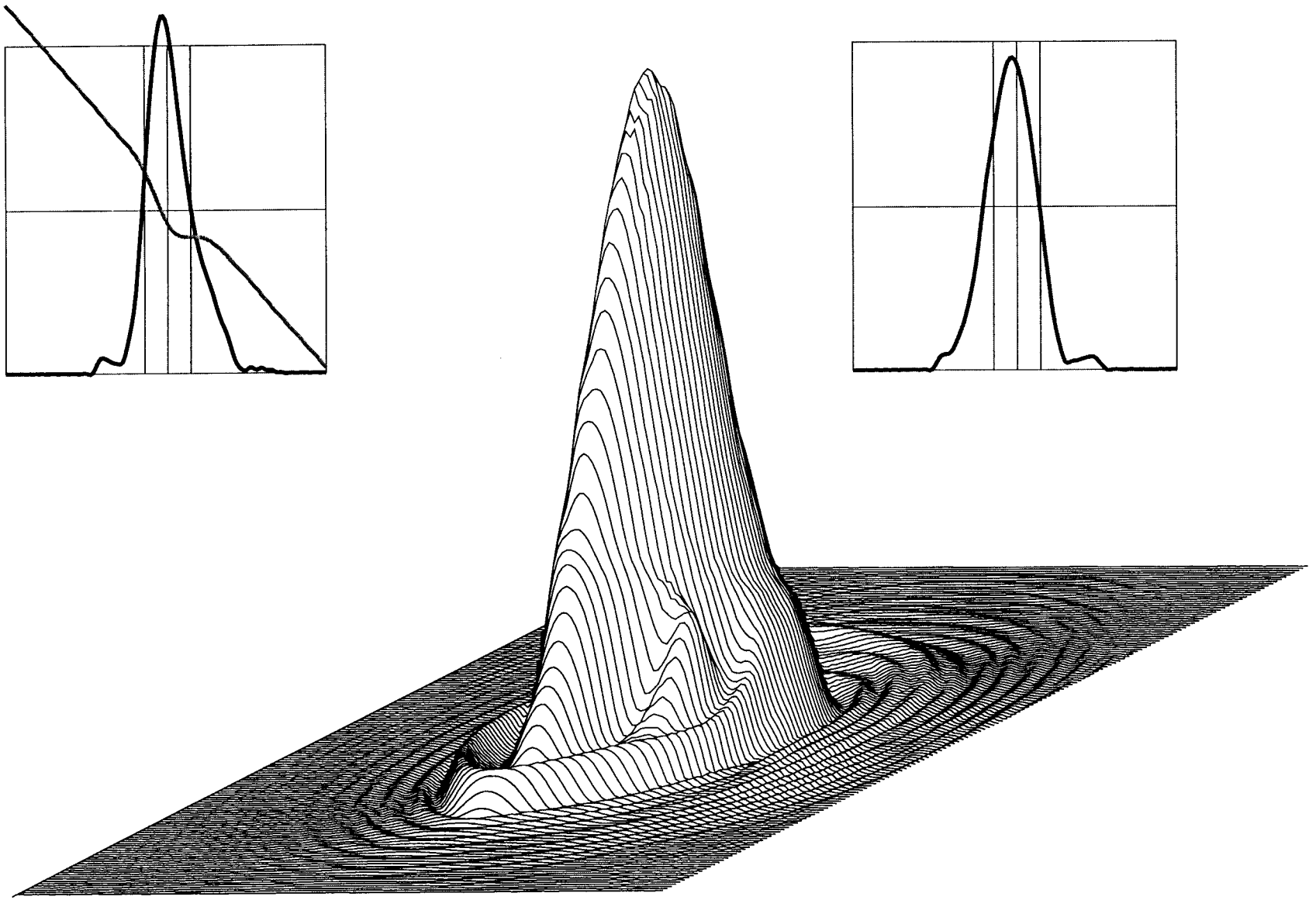

With best wishes, Sasha N. Fri Oct 9 16:39:41 1998 I= 3.00 mu= 1.90 Dx= 0.89 Time=51.98

Fig. 23

A. Mosnier

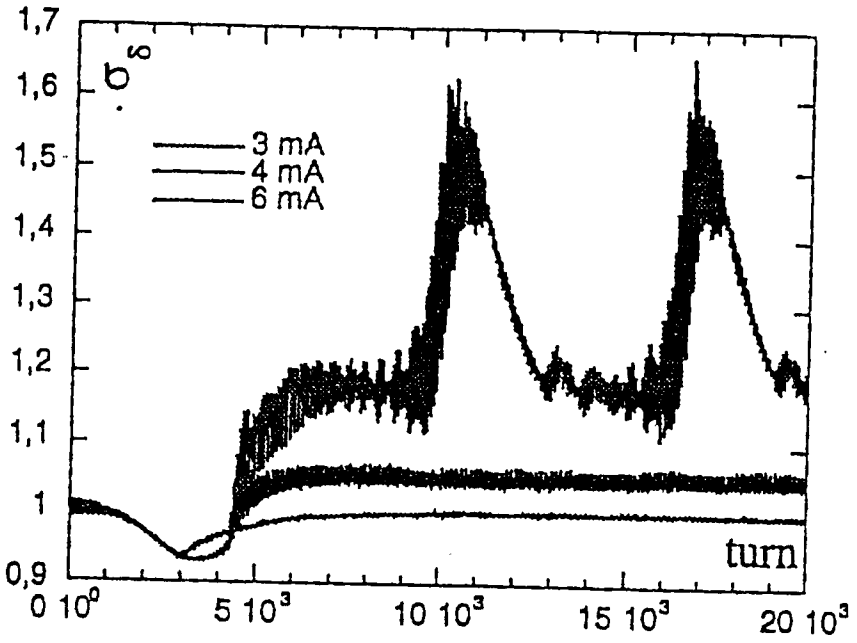

Energy spread widening as a function of the number of turns.

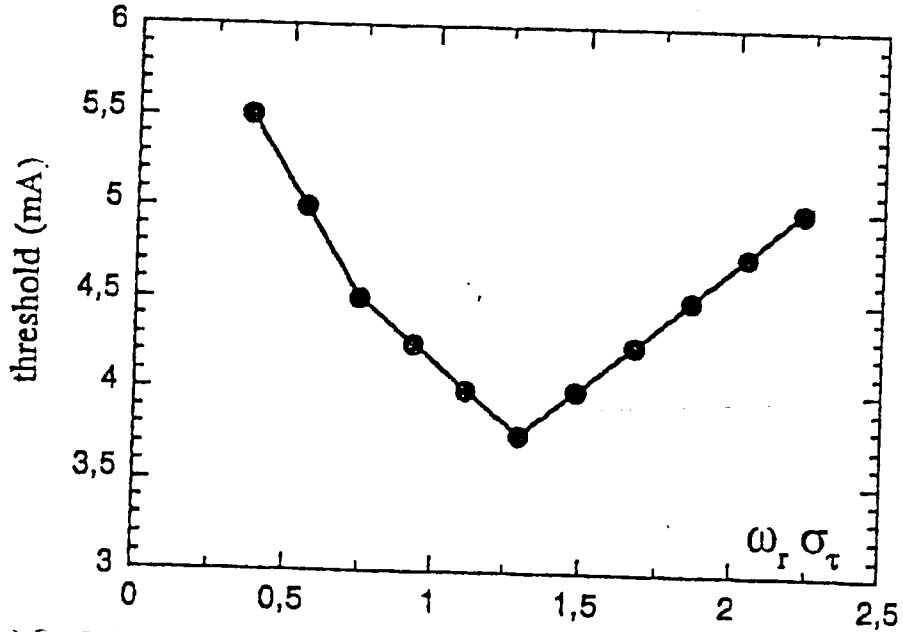

Fig. 22 Microwave instability threshold as function of normalized resonator frequency.

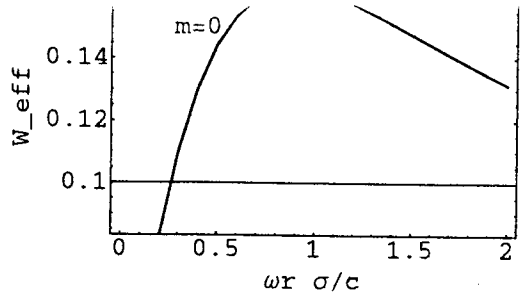

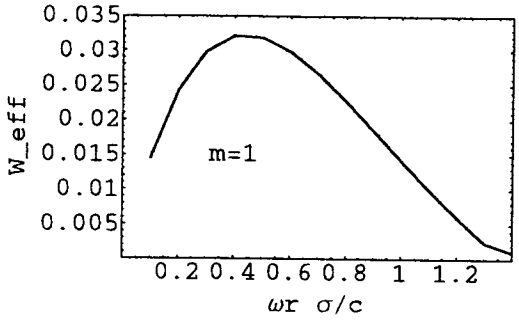

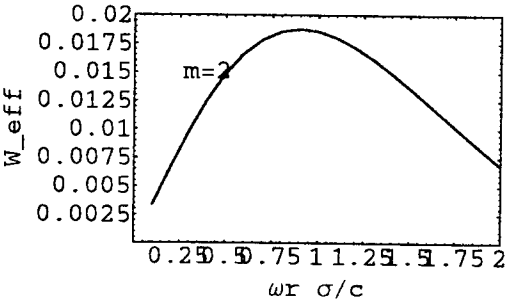

$$\frac{W_{eff}}{R_s} = \frac{1}{\pi}\int_0^\infty \frac{dx}{x}\,\frac{(x/x_\sigma - x_r/x)}{1+(x/x_\sigma - x_r/x)^2}\, e^{-x^2} I_m(x^2)$$

$$x_r = \frac{\omega_r \sigma}{c}$$

$$Z(\omega) = \frac{R_s}{1 - i(\omega/\omega_r - \omega_r/\omega)}$$

$$\frac{W_{eff}}{R_s} \cdot \mathrm{Re}\int_{-\infty}^{\infty} \frac{d\omega}{2\pi}\,\frac{Z(\omega)}{\omega}\int_0^\infty dJ\, e^{-J} J_m^2\left(\frac{\omega\sigma}{c}\sqrt{2J}\right) =$$

I = 3 A. Novokhatsk.

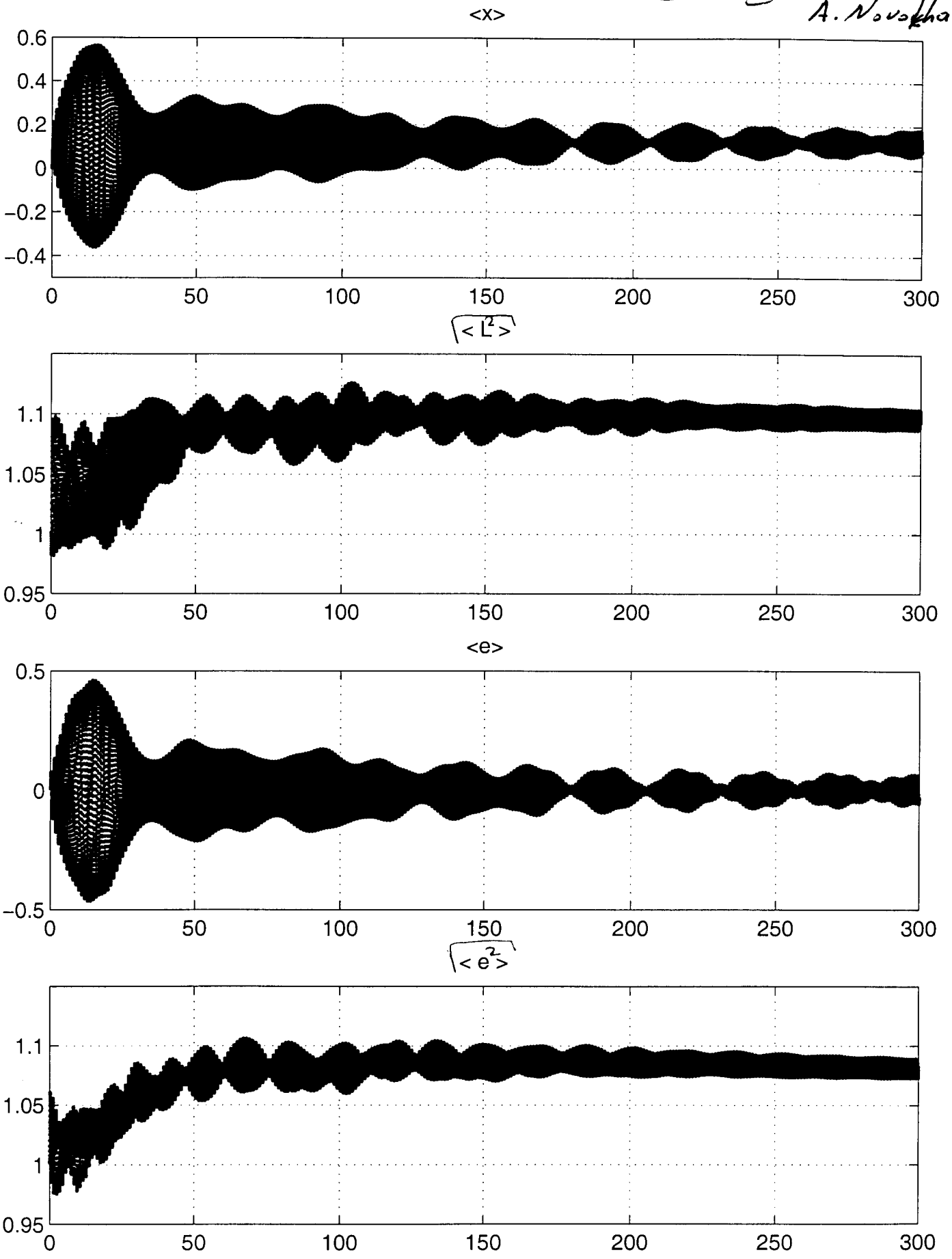

Fig. 24

R. Warnock

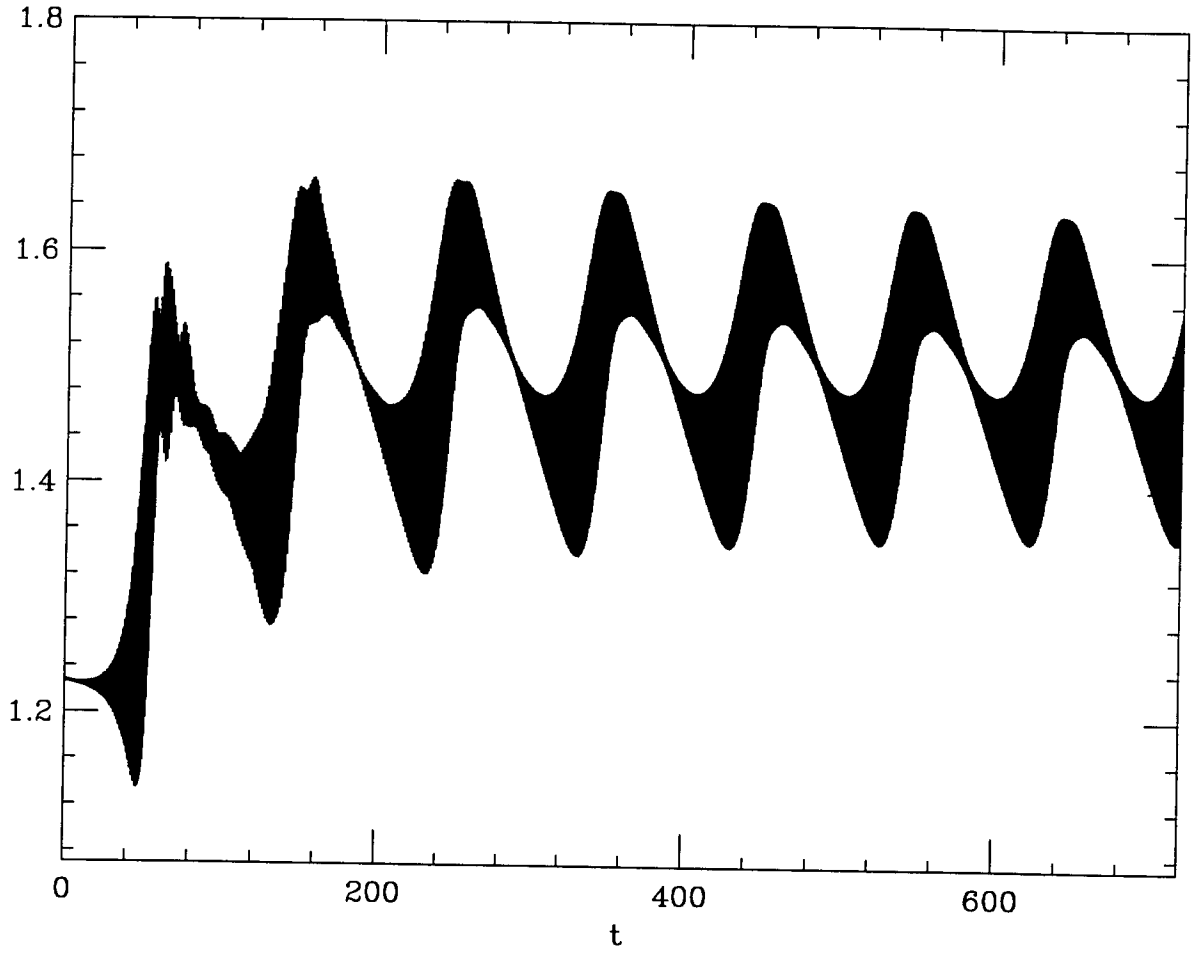

Fig 25

Impedance Issues

1. Main components: RF+RW may be not enough
to describe MW instability
(although SPEAR shows just an opposite example)

2. Small components in the ring may be important.
They may change the character of Z(ω) with σ.

3. For instability in the m-th azimuthal mode,
frequencies ω/c~m/σ may be important

4. BB Q=1 model does not describe well dependence
of $\chi(\sigma)$ and high frequency tail of Z(ω).
Inductive-like model may work better.

5. Summing up contributions of individual components
may over-estimate the total impedance.
Example: periodic structires.
Correlation length $L \sim (2/\pi)(b^2/\sigma)$.

6. Simulations of the whole structures (K. Bane, SLC)
and off-centered beams may become possible
with new tools (Yong Sun et. al., matrices with
dimension 10^6 and multi-processing)

New Issues:

1. RW for small bunches:

W(s)~$s^{-3/2}$ only for $s >> s_0$,
$s_0 = (c\, b\,\hat{}\, 2 / 2\,\pi\sigma_w)^{1/3}$.

$s_0 \sim 20\ \mu$ for Cu 1 cm beam pipe.

2. Rough Surface (K. Bane et.al., G. Stupakov) (A. Novokhatski)

$$\frac{Z}{Z_{RW}} \sim \frac{d^2}{\delta\, l_c}$$

Measurements: $d \sim 0.1\ \mu$, $l_c \sim 100\ \mu$, $\delta \sim 1\ \mu$.

3. CSR

$$W(s) = -\frac{1}{\sqrt{2\,\pi\,\sigma^2}} \left(\frac{L}{R}\right) \left(\frac{R}{3\,\sigma}\right)^{1/3} F(s/\sigma), \quad -0.3 < F < 1.1$$

However, CSR requires $\sigma < (2/\pi)\, b \sqrt{b/\rho}$.

4. Oxide layers:

$l \sim 100$ Å to be compared with $\delta \sim 1\ \mu$ for $\sigma = 1$ cm.
But secondary e- yield may be high.

K. Bane

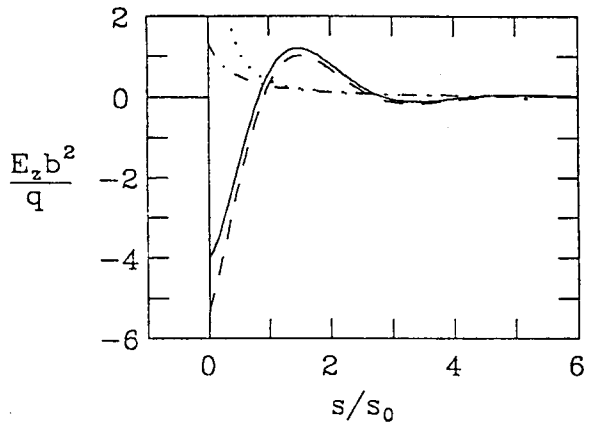

FIGURE 36 The short-range longitudinal resistive wall wakefield (the solid curve). Also shown are the oscillator component (the dashes), the diffusion term (the dotdashes), and the long range solution of E_z [see Eq. (9)] (the dots).

Derbenev et.al.

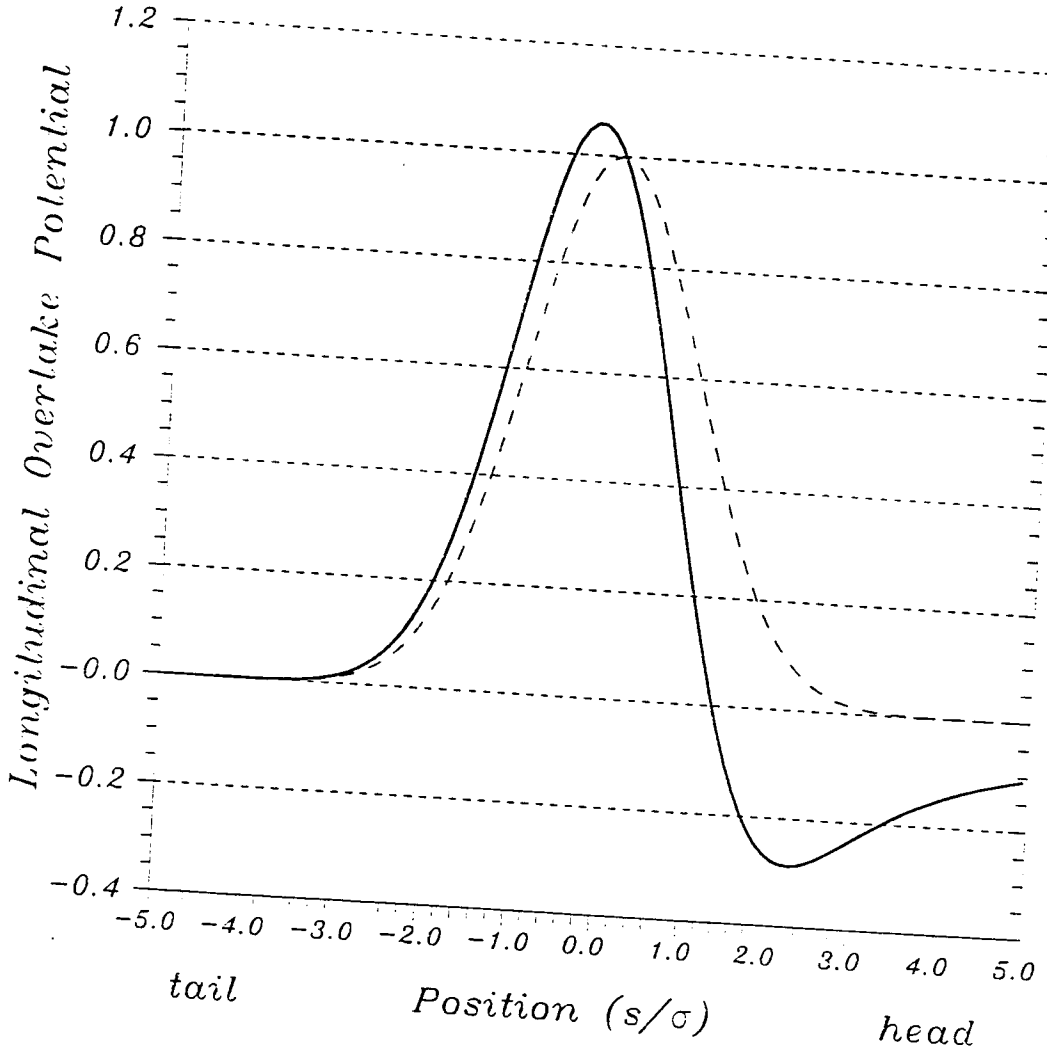

Fig.27 Longitudinal overtake potential $F_0(s/\sigma_s)$ (solid line) for the Gaussian charge distri...

Conclusion

1. Relaxation oscilltions are quite normal nonlinear phenomenon which may be driven by the NB- or BB-impedances, longitudinal and transerse.

2. The most realistic scenario now is the mode interaction with particle trapping due to the change of d.f. by the unstable modes themselves.

3. Qualitative picture and analysis of beam stability based on the linearized Vlasov equation may give guidence for behavior for small rms σ and α .

4. Mode coupling may be both radial or azimuthal depending on the character of the impedance which may depend on rms σ.

5. F-PL solvers may give not only threshold but also describe beam dynamics above the threshold.

7. Smaller σ, (large rf V, fixed α) -stronger instability:

Loss factor (resistive part of Z) increases,
Inductive components may become resistive/capacitive, cmp. SLC DR

6. Impedance of a machine should be constructed with careful modeling of the high-frequency impedance.

However, even a strong single HOM may cause saw-tooth behavior.

7. The next generation of machines may, probably, use the same approach to impedance analysis as it is done today.

References

[1] J. Haissinski, Nuovo Cimento, 18 B, 72, 1973

[2] R. Holtzapple Ph.D. Thesis, Longitudinal Dynamics at the SLAC DR, Hune 1996

[3] A. Ogata et.al., Longitudinal Instability in TRISTAN main ring, European Part. Accel. Conf, Rome, Italy, June 7-11,1998

[4] ,P. Krejcik, et. al., Proc IEEE Part. Accel. Conf., Washington D.C., p. 3240, 1993

[5] B. Podobedov, R. Siemann, Signals from Microwave Unstable Beams in the SLAC Damping Rings, Proceedings of PAC-99, 146, 1999

[6] ,C.Limborg, J. Sebek, Relaxation Oscillations of the synchrotron motion caused by narrow-band impedance, Phys. Rev E, 60, N. 4, p.4823, 10/1999

[7] K. Oide, A mechanism of Longitudinal Instabbility in Storage Rings, KEK Preprint 94-138, 1994

[8] R. Baartman and M. Dyachkov, Proc. IEEE, Part. Accel. Conf. Dallas, 1995

[9] K. Harkay, et al Impedance and the single bunch limit in the APS storage ring, PAC 1998

[10] J. Schonfeld Ann.Phys. 160, 149, 1985

[11] R.E. Meller, Ph.D. Thesis, Statistical Methods for Nonequilibrium Systems with Applications to Beam Dynamics, Cornell 1986

[12] S. Heifets, Phys. Rev. 54, p.2889, 1996

[13] T. O'Neil, Phys. Fluids 8, 2255, 1965

[14] S. Heifets, Nonlinear Mode Coupling and Saw-tooth instability, SLAC-PUB-8242, 9/1999, Workshop on Instabilities in High-Intensity Hadron Beams in Rings, Brookhaven, June 1999

[15] G. V. Stupakov et. al., Dynamics of single bunch instability in accelerators, SLAC-PUB-7377, 12/1996

[16] R. Warnock, A general method for propagation of the phase space distribution with application to the saw-tooth instability, submitted to World Scientific, 2/2000

[17] G. V. Stupakov, Impedance of small obstacle and rough surfaces, SLAC-PUB-7908, August 1998